AWARD NUMBER: W81XWH-18-1-0326

TITLE: Sensitizing ovarian cancer to PARP inhibition by targeting claudin-4 activity

PRINCIPAL INVESTIGATOR: Benjamin Bitler, PhD

CONTRACTING ORGANIZATION: The University of Colorado, Aurora, CO

REPORT DATE: November 2021

TYPE OF REPORT: Final Report

PREPARED FOR: U.S. Army Medical Research and Development Command
Fort Detrick, Maryland 21702-5012

REPORT DOCUMENTATION PAGE

Form Approved
OMB No. 0704-0188

1. REPORT DATE	2. REPORT TYPE	3. DATES COVERED
November 2021	Final Report	15Jul2018-14Jul2021

4. TITLE AND SUBTITLE

Sensitizing ovarian cancer to PARP inhibition by targeting claudin-4 activity

5a. CONTRACT NUMBER
W81XWH-18-1-0326

5b. GRANT NUMBER
OC170228

5c. PROGRAM ELEMENT NUMBER

6. AUTHOR(S)

Benjamin Bitler, PhD

E-Mail: Benjamin.bitler@cuanschutz.edu

5d. PROJECT NUMBER

5e. TASK NUMBER

5f. WORK UNIT NUMBER

7. PERFORMING ORGANIZATION NAME(S) AND ADDRESS(ES)

University of Colorado
Anschutz Medical Campus
Research Complex II (RC2)
12700 East 19th Avenue, 3400D
Aurora, Colorado 80045

8. PERFORMING ORGANIZATION REPORT NUMBER

9. SPONSORING / MONITORING AGENCY NAME(S) AND ADDRESS(ES)

U.S. Army Medical Research and Development Command
Fort Detrick, Maryland 21702-5012

10. SPONSOR/MONITOR'S ACRONYM(S)

11. SPONSOR/MONITOR'S REPORT NUMBER(S)

12. DISTRIBUTION / AVAILABILITY STATEMENT

Approved for Public Release; Distribution Unlimited

13. SUPPLEMENTARY NOTES

14. ABSTRACT

Purpose: To define the mechanisms of claudin-4 induced PARP inhibitor resistance in ovarian cancer.
Scope: The work used ovarian cancer cells, mouse models of ovarian cancer, and primary human tumors to assess claudin-4 expression and response to PARP inhibitors. The findings of the work have broad implications in not only improving understanding on ovarian cancer biology but all in cancers being treated with PARP inhibitors.
Major Findings: We discovered claudin-4 is directly related to DNA damage repair, replication stress, and mitotic spindle assembly. Also, loss of claudin-4 improves sensitivity to PARP inhibitors.

15. SUBJECT TERMS

Ovarian cancer, PARP inhibitors, DNA damage, claudin-4

16. SECURITY CLASSIFICATION OF:			17. LIMITATION OF ABSTRACT	18. NUMBER OF PAGES	19a. NAME OF RESPONSIBLE PERSON
a. REPORT	b. ABSTRACT	c. THIS PAGE			USAMRMC
Unclassified	Unclassified	Unclassified	Unclassified	47	19b. TELEPHONE NUMBER *(include area code)*

Table of Contents

Page

INTRODUCTION: Epithelial ovarian cancer (EOC) is the deadliest gynecological disease and annually accounts for over 140,000 deaths worldwide. High grade serous (HGSOC) comprises about 70% of EOC cases. An emerging therapeutic strategy for HGSOC, poly(ADP) ribose polymerase inhibitors (PARPi) effectively targets homologous recombination (HR) deficient cancers (e.g. BRCA1/2-mutated). Several trials have demonstrated that PARPi response is not entirely dependent on *BRCA1/2* status indicating the need for additional predictive biomarkers. Analyses of HGSOC tumors in The Cancer Genome Atlas (TCGA) revealed a tendency toward mutual exclusivity between *CLDN4* overexpression and *BRCA1/2* mutation and downregulation, indicating low *CLDN4* could potentially predict PARPi response. Claudin-4 (CLDN4) is expressed in approximately 70% of all human EOC tumors and is highly upregulated in carboplatin/paclitaxel resistant ovarian tumor cells. A stable D-amino acid claudin mimic peptide, CMP, was designed to disrupt Claudin-4-protein interactions and was shown to significantly reduce overall tumor burden in a mouse model of HGSOC ovarian cancer. The objectives of this DoD Pilot Award are to establish claudin-4 as novel biomarker that better predicts PARPi response and investigate a therapeutic strategy to sensitizing ovarian tumors to PARPi. This DoD funded research will elucidate the relationship between claudin-4 expression and PARPi sensitivity. The work is anticipated to lay critical foundation to establish the use of claudin-4 as a biomarker and/or therapeutic target in combination with PARP inhibitors to target non-BRCA1/2-mutated HGSOC tumors. The proposed work directly addresses several of the DOD OCRP key priorities. If successful, these findings will have an immediate and long-term impact on EOC patients.

KEYWORDS: PARP inhibitors, high grade serous ovarian cancer, claudin-4,

Overall Project Summary:

Entirety of the DOD Pilot Award Work can be found in Yamamoto TM, Webb PG, Baumgartner HK, Neville M, Behbakht K, Bitler BG. (2021). Loss of Claudin-4 reduces DNA damage repair and increase sensitivity to PARP inhibitors. In review at *Molecular Cancer Therapeutics*. Attached as an appendix.

What were the major goals of the project?

- Determine the sensitivity of cell lines and tumor tissue to PARPi.
    - Percentage completed: 100%
- Determine the effect of claudin-4 on development/reversal of PARPi resistance.
    - Percentage completed: 100%
- Determine the effect of claudin-4 on DNA repair.
    - Percentage completed: 100%
- Determine the effect of CMP co-treatment on PARPi response in vivo.
    - Percentage completed: 100%
- Characterize claudin-4 expression and PARPi sensitivity of patient tumor samples.
    - Percentage completed: 100%

What was accomplished under these goals?

- *Determine the sensitivity of cell lines and tumor tissue to PARPi.*

Previously reported, HGSOC cells lines were authenticated through the University of Arizona TCGA core facility via small tandem repeat analysis. We established Claudin-4 expression in OVCAR8,

OVCAR10, OVCAR4, OVCAR3, and OVCA429. We determined the half maximal inhibitory concentration (IC50) of olaparib and rucaparib in these four HGSOC cell lines. We found that Claudin-4 expressing lines had a lower half maximal inhibitory concentration (IC50) to olaparib compared to cells with low claudin-4 expression. In contrast, response to rucaparib was varied and did not correlate with claudin-4 status (**Figure 1**).

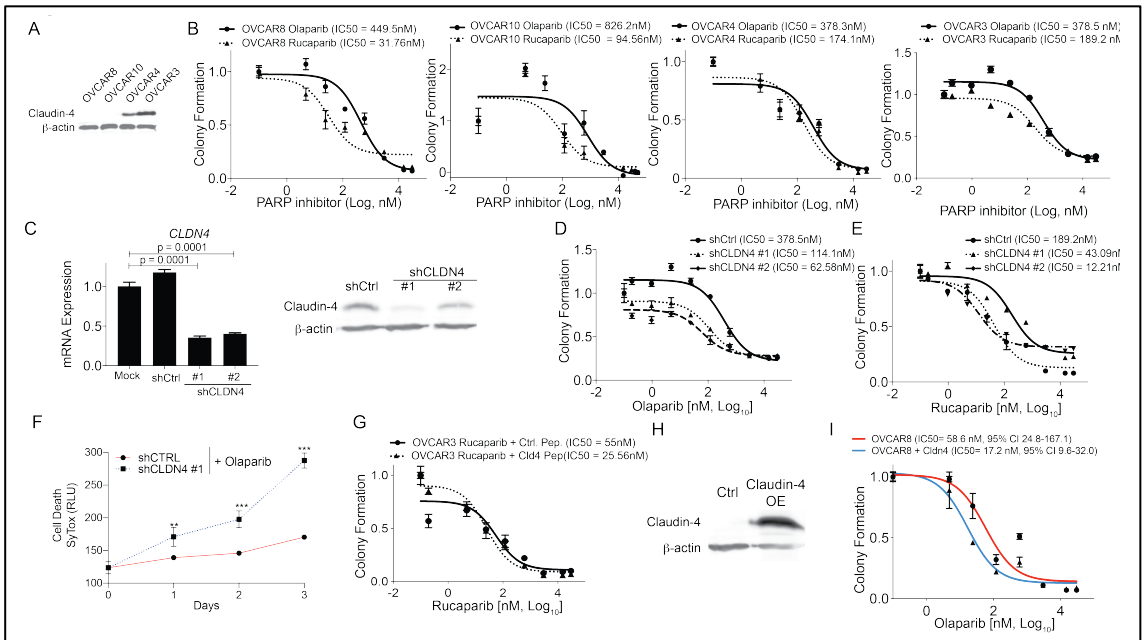

Figure 1. The relationship between Claudin-4 and PARP inhibitor response. A) Immunoblot against Claudin-4 in HGSOC cell lines. **B)** Olaparib and rucaparib (dotted lines) dose response in indicated HGSOC cell lines. **C)** Knockdown of Claudin-4 (*CLDN4*) in OVCAR3 cells, mRNA (Internal Control = 18S) and protein (Loading Control = β-actin). **D)** Olaparib and rucaparib **(E)** dose response in shCLDN4 cells. **F)** Cell death of OVCAR3 shCTRL and shCLDN4 cells with SyTox assay over time. **p<0.01, ***p<0.001. **G)** Dose response of rucaparib with control peptide (Ctrl. Pep.) or with CMP (Cld4 Pep., 400μM). **H)** Immunoblot of Claudin-4 in OVCAR8 Claudin-4 overexpressing cells. **I)** Olaparib dose response in OVCAR8 cells with or without Claudin-4 overexpression. Error bars = S.E.M. Statistical Test, multicomparison ANOVA with Tukey (C), Two-way ANOVA (F). **p<0.01, ***p<0.001

- *Determine the effect of claudin-4 on development/reversal of PARPi resistance.*

The major findings for this task are that modulation of Claudin-4 resensitized HSGOC cells to PARP inhibition. Interestingly, the effect is cell line dependent in which knocking Claudin-4 down sensitizes OVCAR3 cells but overexpressing it in OVCAR8 cells sensitizes cells to olaparib. Specific cell line attributes that contribute to PARP inhibitor response are further interrogated in the next task. Given claudin-4 expression is present in

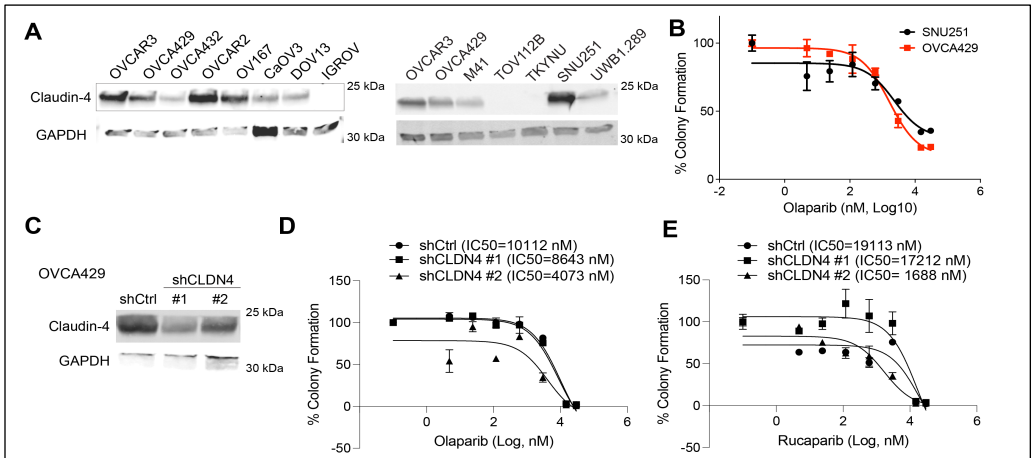

Figure 2. Assessing claudin-4 expression in HGSOC cell lines and confirming OVCAR3 results. A) Protein isolated from 13 HGSOC cells was immunoblotted for claudin-4. Loading control, GAPDH. **B)** Olaparib dose response in OVCA429 and SNU251 claudin-4 expressing cells. **C)** OVCA429 cells transduced with shControl and shCLDN4 immunoblotted for claudin-4. Loading control, GAPDH. **D)** Olaparib dose response in OVCA429 shCtrl and shCLDN4. **E)** Rucaparib dose response in OVCA429 shCtrl and shCLDN4. Error bars, SEM. Statistical test, non-linear regression.

greater than 70% of HGSOC tumors, we focused on knocking down claudin-4 in additional HGSOC claudin-4 expressing cell lines. We screened 13 HGSOC cell lines and observed OVCAR2, SNU251, and OVCA429 cells had high claudin-4 expression (**Figure 2A**). We determined olaparib response in SNU251 and OVCA429 cells (**Figure 2B**). Then, we confirmed the OVCAR3 data and observed that loss of claudin-4 in OVCA429 cells reduced the IC50 of olaparib and rucaparib (**Figure 2C-E**).

- *Determine the effect of claudin-4 on DNA repair.*

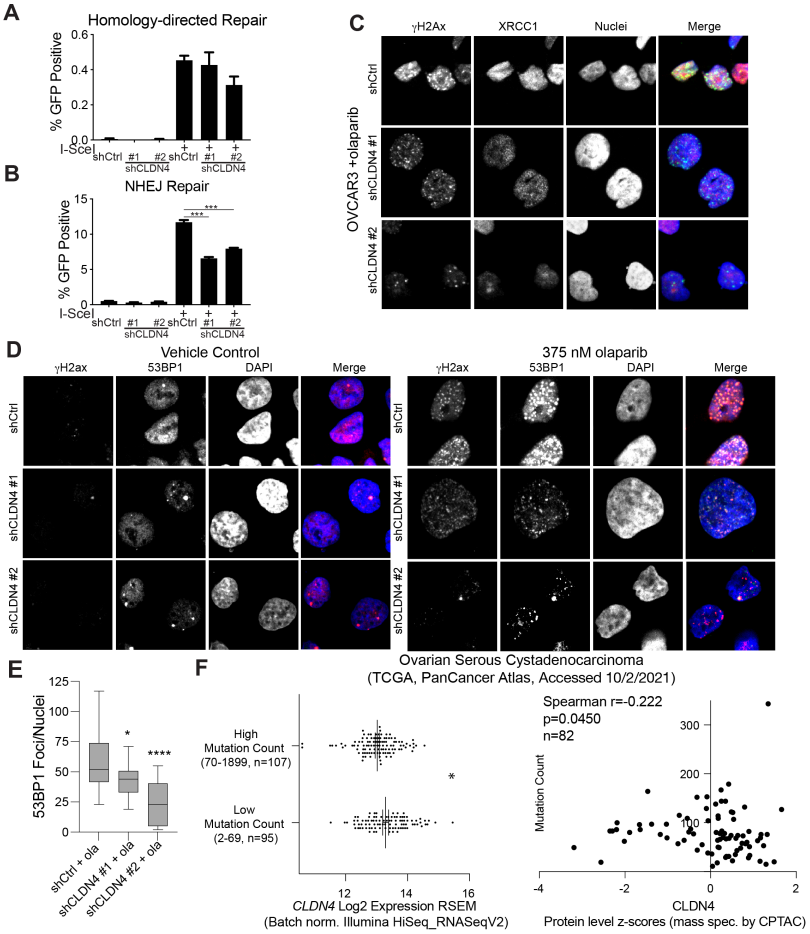

Figure 3. Claudin-4 knockdown inhibits non-homologous end joining and reduces 53BP1 foci formation. A) Homology-directed DNA repair activity measured in OVCAR3 shCtrl and shCLDN4 (#1 and #2) cells transfected without I-SceI and with I-SceI. **B)** Non-homologous end-joining DNA repair activity measured in OVCAR3 shCtrl and shCLDN4 (#1 and #2) cells transfected without I-SceI and with I-SceI. **C)** OVCAR3 shCtrl and shCLDN4 (#1 and #2) cells treated with control [not shown] or 375 nM olaparib used for immunofluorescence against gH2ax (green) and XRCC1 (red). Nuclei stained using DAPI (blue). **D)** OVCAR3 shCtrl and shCLDN4 (#1 and #2) cells treated with vehicle control or 375 nM olaparib used for immunofluorescence against gH2ax (green) and 53BP1 (red). Nuclei stained using DAPI (blue). **E)** Same as E, quantification of 53BP1 foci per nuclei from five field of views. **F)** Low (2-69, n=95) and high (70-1899, n=107) mutation count from TCGA ovarian cancer tumors (x-axis) compared to claudin-4 mRNA expression (y-axis). Claudin-4 protein expression (CPTAC) versus Mutation count (y-axis) from 82 HGSOC TCGA tumors. Experimental performed at minimum in triplicate. Error bars, SEM. Statistical Test, one way ANOVA with multicomparison correction (A, B, E, F) or unpaired t-test (F) or Spearman Correlation (F). *p<0.05, **p<0.01, ***p<0.001, ****p<0.0001.

To assess whether Claudin-4 is involved in DNA repair processes we propose to examine functional DNA repair process, expression of DNA repair enzymes, replication stress, and markers of DNA damage. Previously reported, to assess Claudin-4 contribution to DNA damage repair, we used OVCAR3 shControl and shCLDN4 (#1 and #2) cells. The loss of claudin-4 expression did not significantly alter homology-directed repair activity. However, the loss of claudin-4 significantly inhibited NHEJ repair activity (**Figure 3A-B**). Consistently, loss of claudin-4 did not impact gammaH2Ax induction, but significantly inhibited 53BP1 foci formation following treatment with olaparib (**Figure 3C-E**). Considering claudin-4's novel role in DNA repair, in TCGA human HGSOC tumors we examined the mutation count based on claudin-4 expression. We observed that both the mRNA and protein expression of claudin-4 correlated to mutation count, with lower claudin-4 expression correlating to higher mutational count (**Figure 3F**).

While PARPi response is largely dependent on DNA damage response, since the start of this DOD Pilot award replication stress has become and accepted mechanism of PARPi action [1-4]. Therefore, in addition to DNA damage (yH2Ax) we also examined replication stress using phosphor-Serine 8

Replication Protein A (phosphor-RPA) following olaparib treatment via yH2Ax in OVCAR3 shControl and OVCAR3 shCLDN4 (#1 and #2). In a similar experiment, we performed a time course (0 to 11 hrs) in shControl and shCLND4 #2 cells that were irradiated to induce DNA damage. In contrast to the 72 hour time course, we observed that phosphor-RPA remained elevated in the claudin-4 knockdown cells compared to the shCtrl cells. Similarly, the induction of gammaH2Ax levels were blunted in the shCLDN4 cells compared to shCtrl cells, especially at the 8, 10, and 11 hour time points (**Figure 4**). Taken together, these data suggest that claudin-4 contributes to DNA damage response. Loss of claudin-4 inhibits NHEJ, attenuates yH2Ax expression, and promotes replication stress – all of which are likely to contribute to PARPi response.

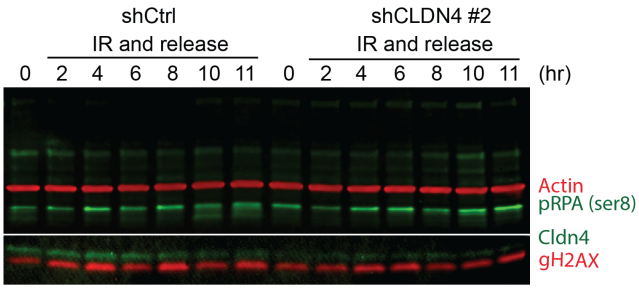

Figure 4. Claudin-4 regulation of DNA damage repair and replication stress. shCtrl or shCLDN4 (#2) OVCAR3 cells irradiated (5 Gy) and protein was collected at indicated time points. Protein used for immunoblot for for gammaH2Ax, pRPA ser8, and Claudin-4. Loading control, beta-actin.

Using an unbiased approach, we assessed differential response of 126 FDA approved chemotherapeutic agents in OVCAR3 shCtrl and shCLDN4 cells. Consistent with our data showing that loss of claudin-4 increased the sensitivity of HGSOC cells to DNA damaging agents, we observed that claudin-4 loss increased the sensitivity of DNA damaging agents (e.g., alkylating agents) (**Figure 5**). These data will be incorporated into the manuscript in preparation.

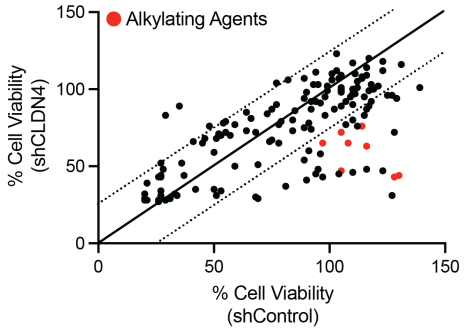

Figure 5. Claudin-4 knockdown cells are more responsive to DNA damaging agents. OVCAR3 shControl and shCLDN4 #1 were plated in a 96 well format and treated with 1 uM of 126-FDA approved chemotherapies. Cells were incubated for 72 hrs, fixed for crystal violet, and absorbance was measured as a surrogate for cell viability. Red Dots = Alkylating agents. Dotted lines -/+ 25% error.

Determine the effect of CMP co-treatment on PARPi response with in vivo.

Novel and rationale combinatorial therapeutics strategies are needed to improve ovarian cancer outcomes. We previously demonstrated that targeting Claudin-4 with a mimetic peptide (CMP) significantly inhibited tumor progression [5]. Based on the reverse phase protein array knockdown of Claudin-4 correlates to the loss of several DNA repair proteins suggesting that treatment with CMP could promote a BRCAness phenotype and increase tumor sensitivity to olaparib. Our previous annual report described that CMP in combination with olaparib induced apoptosis. To confirm the *in vitro* findings of claudin-4 knockdown increasing PARP

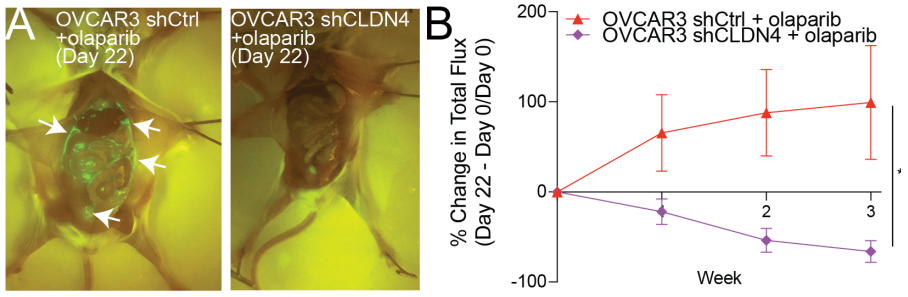

Figure 6. Claudin-4 knockdown tumors are more responsive to PARPi. OVCAR3 GFP/Luciferase cells were transduced with shCtrl (n=7) or shCLDN4 (n=5). Cells were injected IP into NSG mice and allowed to establish for 4 weeks. Mice were randomized using a random number generator and treated for 21 days with daily olaparib (50 mg/kg). Tumor progression was monitored via in vivo imaging. **A)** Representative images of tumor bearing mice at day 22. White arrows = GFP positive tumors. **B)** Tumor growth shown as % change. Error bars, SEM. Statistical test, unpaired t-test with Welch's correction. *p=0.014. F-test, p<0.0001.

inhibitor sensitivity, we compared the anti-tumor response of olaparib in OVCAR3 shCtrl versus shClaudin-4 tumors. In an immune-compromised model we found that claudin-4 knockdown OVCAR3-derived tumors were more responsive to olaparib compared to claudin-4 expressing tumors (**Figure 6A-B**). Importantly, knocking down claudin-4 followed by olaparib treatment resulted in tumor regression (**Figure 6B**).

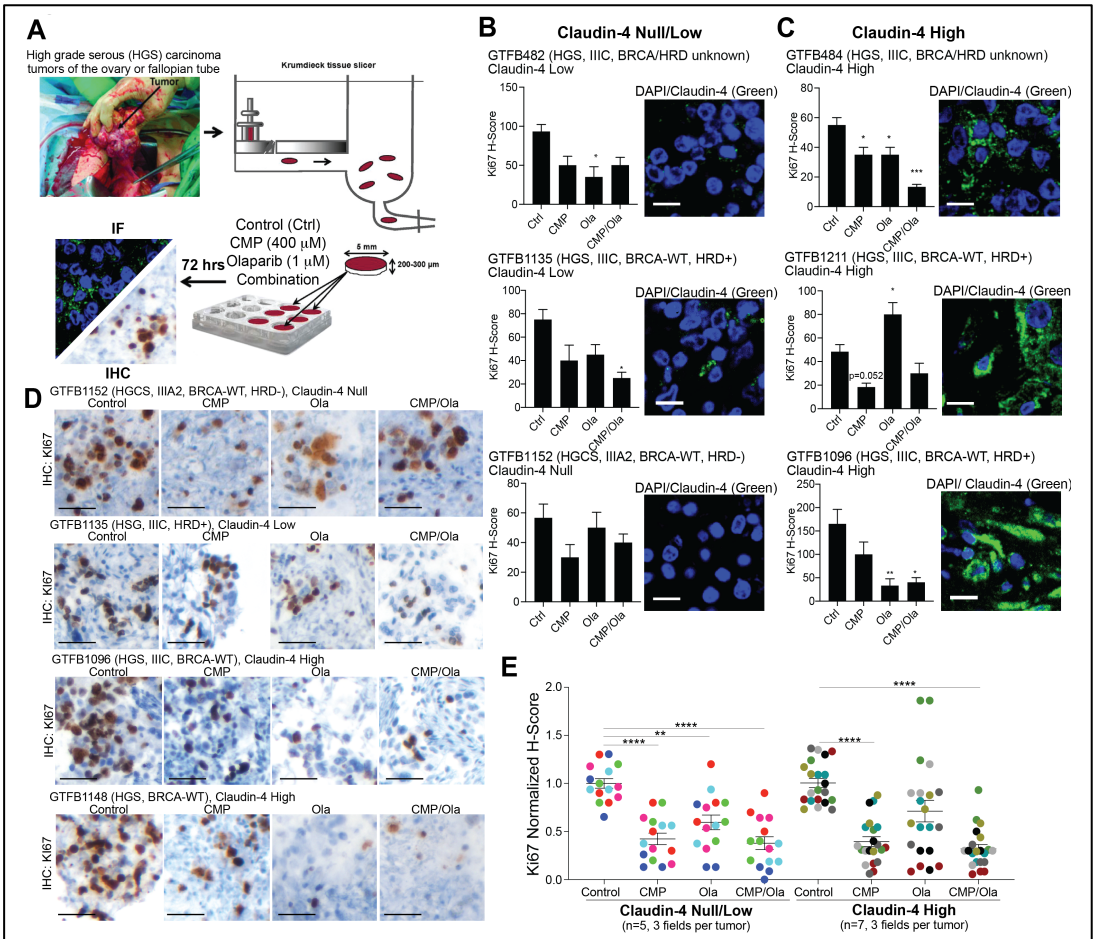

Figure 7. Olaparib and inhibition of claudin-4 inhibit proliferation of primary ovarian cancer tumors. A) Workflow of the ex vivo experiments using primary tumor tissue. Primary tumors were classified as claudin-4 null/low or claudin-4 high based on immunofluorescence (IF, claudin-4, green and nuclei, DAPI). IHC against Ki67 was completed in all the tumors, tumors were de-identified, and a histology score (H-score) was calculated based on intensity of Ki67 signal and percentage of tumor cells from at least three fields of view. **B)** Representative H-score and claudin-4 IF for claudin-4 null/low expressing ovarian cancer tumors. **C)** Representative H-score and claudin-4 IF for claudin-4 high expressing ovarian cancer tumors. **D)** Representative Ki67 images of claudin-4 null/low and high expressing ovarian cancer tumors (Scale bar, 50 microns). **E)** Normalized Ki67 H-score based control (Ctrl) treated tumors for all the claudin-4 null/low (N=5) and high (N=7) expressing serous ovarian tumors. Three fields from each tumor were analyzed and each tumor is represented by three matched colored spots. Error bars, SEM. Statistical test, one way ANOVA with multicomparison correction. *p<0.05, **p<0.01, ***p<0.001, ****p<0.0001.

- *Characterize claudin-4 expression and PARPi sensitivity of patient tumor samples.*

To assess the impact of combining CMP with olaparib we utilized *ex vivo* cultures of primary tumors samples. To date, we have examined CMP and olaparib treatment in ten primary tumors. Primary tumors were obtained within one hour from the operating room and uniformly sectioned on a Krumdieck Tissue Slicer (**Figure 7A**). Tumor sections were treated with control, olaparib [1 μM], CMP [400 μM], or in combination for 72 hrs. Sections were fixed, embedded, sectioned, and used for IHC analysis against claudin-4, an apoptosis marker (Cleaved caspase 3, CC3) and proliferation marker (Ki67) (**Figure 7A**). During the course of the no-cost extension, we were able to conduct four additional ex vivo studies. Figure 4 represents the final figure that will be incorporated into the manuscript under preparation.

We observed that tumors without claudin-4 expression had an improved anti-proliferative response compared to HGSOC tumors that expressed high levels of claudin-4. CMP and olaparib treatment reduced Ki67 expression in most of the HGSOC tumors, with a more robust response observed in the claudin-4 expressing tumors (**Figure 7B-E**). Previously reported, using the tissue microarray (TMA) constructed during the first year of this DOD award, we examined overall survival in patients with genetic testing that confirmed no BRCA-mutations that had low or high claudin-4 expression. We observed that high claudin-4 expression conveyed a worse overall survival (Hazard Ratio: 3.056, 95% CI 0.88-10.59) (**Figure 8A-B**). Taken together with the in vivo tumor models, targeting claudin-4 in combination with olaparib had anti-proliferative effects. Further, there is an indication that combining olaparib with CMP in BRCA-wildtype tumors could be effective at inducing apoptosis.

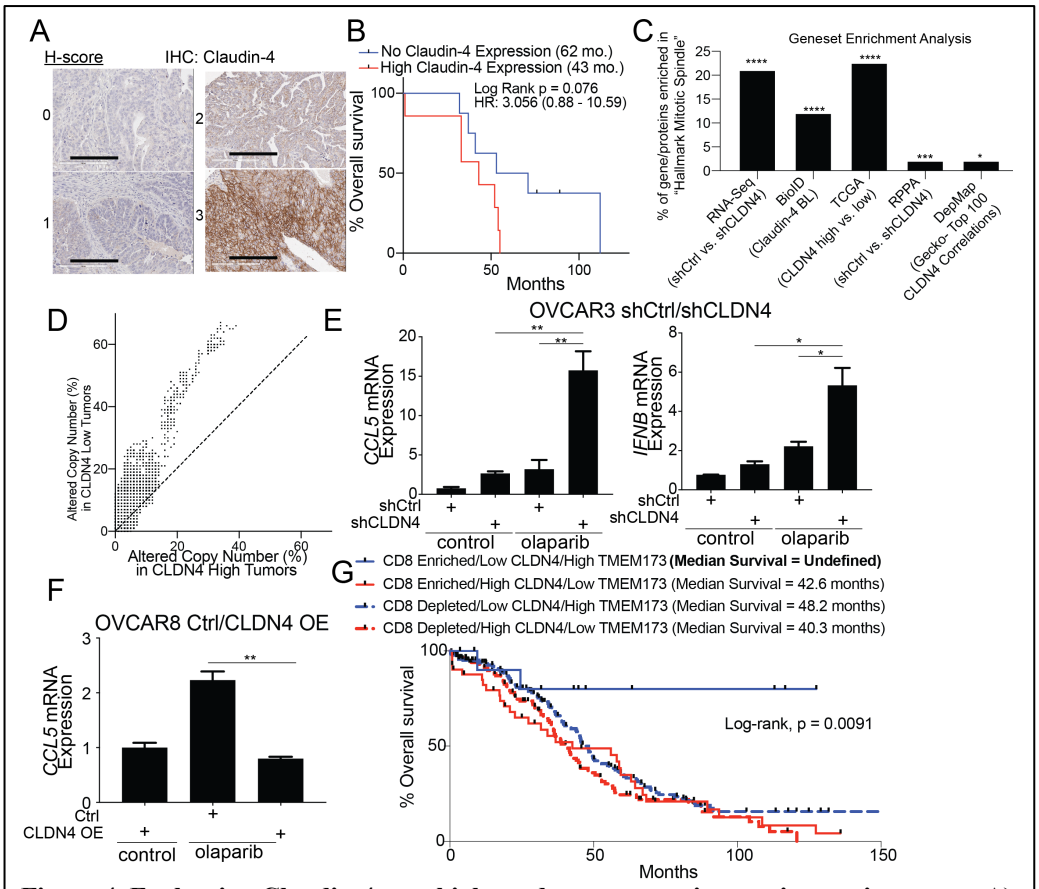

Figure 4. Evaluating Claudin-4 on a high grade serous carcinoma tissue microarray. A) A tissue microarray of primary ovarian cancer tumors was used for immuno-histochemistry (IHC) against Claudin-4. **B)** Kaplan-Meier curve of patients that had known BRCA-wildtype tumors with no claudin-4 vs. high claudin-4 expression. **C)** OVCAR3 shCtrl and shCLDN4 cells used for RNA-seq/RPPA. Significant (adj. $p<0.5$) "hits" were enriched for mitotic spindle assembly. OVCAR8/OVCAR3 cells transduced with claudin-4 biotin ligase (BioID) and claudin-4 interacting proteins enriched for mitotic spindle assembly. In EOC TCGA tumors, high claudin-4 expression correlated to genes associated with mitotic spindle assembly. **D)** From TCGA data, frequency of copy number changes in *CLDN4* low (y-axis) and *CLDN4* high (x-axis) tumors. **E)** OVCAR3 shCtrl and shCLDN4 were treated with 625 nM of olaparib. RNA was extracted and CCL5 and IFNB expression measured with qPCR. Internal control, *GAPDH*. **F)** Same as C, with OVCAR8 Ctrl and Claudin-4 overexpressing (CLDN4 OE) were treated with olaparib. **G)** Overall survival Kaplan-Meier curve of patients based on claudin-4 (*CLDN4*), STING (*TMEM173*) and CD8 levels. Statistical tests, hypergeometric distribution (C), multicomparison ANOVA, Tukey correction (E-F). *$p<0.05$, **$p<0.01$. Error bars= S.E.M.

Previously reported, we performed several unbiased approaches to determine claudin-4's interactome (BioID), transcriptome (TCGA and RNA-seq), and signaling (Reverse phase protein array). In all of these datasets, we observed that claudin-4 is significantly associated with mitotic spindle assembly (**Figure 8C**). Suggestive of aberrant mitotic progression, in TCGA tumors, the loss claudin-4 is significantly correlated to fewer copy number changes (**Figure 8D**). These data suggest that claudin-4's potentially contributes to mitotic spindle assembly and mitotic progression. A consequence of aberrant mitotic progression is increasing DNA damage and the generation of micronuclei, both of which can activate the cGAS/STING pathway and anti-tumor immunity. We confirmed that the loss of

claudin-4 exacerbated PARPi-induced cGAS/STING activation measured through known target genes, *IFNB* and *CCL5* (**Figure 8E**). Conversely, restoring claudin-4 expression blunted cGAS/STING activation (**Figure 8F**). Next, we evaluated claudin-4 and STING (TMEM173) expression in HGSOC tumors with or without CD8+ T cell infiltration. Strikingly, loss claudin-4 and high TMEM173 expression in tumors with CD8+ T cell conveys a dramatic positive prognosis, with no median survival calculable! (**Figure 8G**). We have potentially uncovered a novel function of claudin-4 in regulating cGAS/STING activation and anti-tumor immunity.We have potentially uncovered a novel function of claudin-4 in regulating cGAS/STING activation and anti-tumor immunity. This is the subject of the TEAL Expansion Award.

Conclusions

In conclusion, during the first two years of the DoD Pilot Award we have made substantial progress in characterizing the relationship between Claudin-4 and PARP inhibitor response. We have discovered novel links to DNA damage response, replication stress, and PARP inhibitor sensitivity. We currently have a publication under review at *Molecular Cancer Therapeutics*. Further, we have developed a TEAL Expansion award and was awarded the expansion award to follow-up on the contribution of claudin-4 in mitotic progression and cGAS/STING activation.

- **What opportunities for training and professional development has the project provided?**

- Nothing to report

- **How were the results disseminated to communities of interest?**

- Nothing to report

- **What do you plan to do during the next reporting period to accomplish the goals?**

- Nothing to report. We are on track and continue to utilize the statement of work to gauge our progress and time to project completion.

IMPACT:

- **What was the impact on the development of the principal discipline(s) of the project?**

- The findings from the *ex vivo* experiments and TMA will have a significant impact on the field of HGSOC response to PARP inhibitors, specifically we expect to make an impact in the fields of replication stress, DNA damage repair, cell cycle regulation, and Wnt/beta-catenin regulation. Furthermore, our data suggests that elevated Claudin-4 expression would be a good prognostic indicator in the context of PARP inhibitor response. The no-cost extension year of the DoD Pilot award proved to be confirmatory of our results and have allowed us to expand our findings into a mouse model and additional primary tumors.

- **What was the impact on other disciplines?**

- We have started to collaborate with Dr. Julie Lang. Dr. Lang is an expert in humanized mouse models and she is a co-investigator on the TEAL expansion. She will be instrumental in extending our findings into immune intact models.

- **What was the impact on technology transfer?**

- Nothing to report

- **What was the impact on society beyond science and technology?**

- Nothing to report

CHANGES/PROBLEMS:

- **Changes in approach and reasons for change**

- Nothing to report

- **Actual or anticipated problems or delays and actions or plans to resolve them**

- An unanticipated problem was the COVID19 pandemic and the resulting temporary shutdown of both clinical research and animal research projects. During the no-cost extension we did not experience any additional problems.

- **Changes that had a significant impact on expenditures**

- Nothing to report

- **Significant changes in use or care of human subjects, vertebrate animals, biohazards, and/or select agents**

- Nothing to report

- **Significant changes in use or care of human subjects**

- Nothing to report

- **Significant changes in use or care of vertebrate animals.**

- Nothing to report

- **Significant changes in use of biohazards and/or select agents**

- Nothing to report

PRODUCTS:

- **Publications, conference papers, and presentations**

- **Journal publications for entire award period:**

1. Wheeler LJ, Watson ZL, Qamar L, Yamamoto TM, Post MD, Berning AA, Spillman MA, Behbakht K, and **Bitler BG** (2018). CBX2 identified as driver of anoikis escape and dissemination in high grade serous ovarian cancer. *Oncogenesis*. Nov 26;7(11):92. PMID: 30478317. Cited by 32. Acknowledgement of federal support – YES

2. Watson L and **Bitler BG** (2019). Type I protein arginine methyltransferases overexpression promotes transformation and potentiates Her2/Neu-driven tumorigenesis. Invited Commentary. *Cancer Research*. 2019 Jan 1;79(1):3-4. PMID: 30602621. Cited by 1.

3. Breed C, Hicks D, Webb P, Galimanis C, **Bitler BG**, Behbakht K, and Baumgartner H (2019). Ovarian Tumor Cell Expression of Claudin-4 Reduces Apoptotic Response to Paclitaxel. *Molecular Cancer Research* Mar;17(3):741-750. PMID: 30606772. Cited by 6. Acknowledgement of federal support – YES

4. Dahl E, Buj R, Leon K, Newell J, **Bitler BG**, Snyder N, and Aird KM (2019). Targeting IDH1 as a pro-senescent therapy in high-grade serous ovarian cancer. *Molecular Cancer Research*. ePub May 20. PMID: 31110157. Cited by 9. Acknowledgement of federal support – YES

5. Yamamoto TM, McMellen A, Watson ZL, Aguilera J, Ferguson R, Nurmemmedov E, Thakar T, Moldovan GL, Kim H, Cittelly DM, Wilson H, Behbakht K, Sikora MJ, and **Bitler BG** (2019). Targeting Wnt Signaling To Overcome PARP Inhibitor Resistance. *Molecular Carcinogenesis.* ePub Jun 10. PMID: 31219654. Cited by 5. Acknowledgement of federal support – YES

6. Ramzan AA, **Bitler BG**, Hicks D, Barner K, Qamar L, Behbakht K, Powell T, Jansson T, Wilson H (2019). Adiponectin receptor agonist AdipoRon induces apoptotic cell death and suppresses proliferation in human ovarian cancer cells. *Mol. Cell Biochem*. ePub Jul 10. PMID: 31292831. Cited by 10.

7. Wheeler LJ, Watson ZL, Qamar L, Yamamoto TM, Sawyer BT, Sullivan KD, Khanal S, Joshi M, Ferchaud-Roucher V, Smith H, Vanderlinden LA, Brubaker SW, Kim H, Espinosa JM, Richer JK, and **Bitler BG** (2019). Multi-omic approaches identify metabolic and autophagy regulators important in ovarian cancer dissemination. *iScience*. ePub Aug 6. PMID: 31437751. Cited by 14. Acknowledgement of federal support – YES

8. Park PH, Yamamoto TM, Watson ZL, Li H, Alcivar A, Bing Xia B, Wang Y, Bernhardy AJ, Turner KM, Kossenkov A, Behbakht K, Casadei S, Swisher EM, Mischel PS, Johnson N, and **Bitler BG** (2019). Amplification of the mutation-carrying BRCA2 allele promotes RAD51 loading and PARP inhibitor resistance in the absence of reversion mutations. *Molecular Cancer Therapeutics*. ePub Oct. 1st. PMID: 31575654. Cited by 15. Acknowledgement of federal support – YES

9. Smith LP, **Bitler BG**, Richer JK, Christenson JL (2019). Tryptophan Catabolism in Epithelial Ovarian Carcinoma. *Trends in Cancer Research.* 14:1-9. PMID: 31736606. Cited by 5.

10. Rao DM, Shackleford MT, Bordeux EK, Sottnik JL, Yamamoto TM, Wellberg EA, **Bitler BG**, and Sikora MJ. (2019). WNT4 and WNT3A activate cell autonomous Wnt signaling independent of PORCN or secretion. *Journal of Biological Chemistry*. Nov 18. pii: jbc.RA119.009615. PMID: 31740580. Cited by 4. Acknowledgement of federal support – YES

11. Watson ZL, Yamamoto YM, McMellen A, Kim HM, Wheeler LJ, Post M, Behbakht K, and **Bitler BG** (2019). Histone methyltransferases EHMT1 and EHMT2 (GLP/G9A) maintain PARP inhibitor resistance in high grade serous ovarian carcinoma. *Clinical Epigenetics*. Nov 27;11(1):165. PMID: 31775874. Cited by 17. Acknowledgement of federal support – YES

12. Li J, Wang W, Zhang Y, Cieślik M, Guo J, Tan M, Green MD, Wang W, Lin H, Li W, Wei S, Zhou J, Li G, Jing X, Vatan L, Zhao L, **Bitler BG**, Zhang R, Cho KR, Dou Y, Kryczek I, Chan TA, Huntsman D, Chinnaiyan AM, and Zou W (2019). Epigenetic driver mutations in ARID1A shape cancer immune phenotype and immunotherapy. *The Journal of Clinical Investigation*. ePub Feb 6th. PMID: 32027624. Cited by 35.

13. Sawyer BT, Qamar L, Yamamoto TM, McMellen A, Watson ZL, Powell T, Richer JK, Behbakht K, Schlaepfer IR*, and **Bitler BG***. Targeting fatty acid oxidation to promote anoikis and inhibit ovarian cancer progression (2020). *Co-corresponding authors. *Mol. Cancer Res*. Mar 20:molcanres.1057.2019. doi: 10.1158/1541-7786.MCR-19-1057. PMID: 32198139. Cited by 12. Acknowledgement of federal support – YES

14. McMellen A, Woodruff ER, Corr BR, **Bitler BG**, and Moroney MR. (2020). Wnt Signaling in Gynecologic Malignancies. *International Journal of Molecular Sciences*. Jun 16;21(12):E4272. doi: 10.3390/ijms21124272. PMID: 32560059. Cited by 15.

15. Jordan KR*, Sikora MJ*, Slansky JE, Minic A, Richer JK, Moroney MR, Hu J, Wolsky RJ, Watson ZL, Yamamoto TM, Costello JC, Clauset AG, Behbakht K, Kumar TR, and **Bitler BG**. (2020). The capacity of the ovarian cancer tumor microenvironment to integrate inflammation signaling conveys a shorter disease-free interval. *Clinical Cancer Research*. ePub Sept. 14th DOI:10.1158/1078-0432.CCR-20-1762 *Co-first authors. PMID: 32928797. Cited by 5. Acknowledgement of federal support – YES

16. Bapat J and **Bitler BG**. (2021). Chapter: The intersection of anoikis resistance and fatty acid metabolism in cancer. Book - Anoikis - How the extracellular matrix regulates life-or-death decisions. Editor, Frisch S. Publisher, Springer Nature Switzerland AG.

17. Moroney MR, Woodruff E, Qamar L, Bradford AP, Wolsky R, ***Bitler BG**, Corr BR. (2021) Inhibiting Wnt/beta-catenin in CTNNB1-mutated endometrial cancer. *Molecular Carcinogenesis*. 2021 May 26. doi: 10.1002/mc.23308. Online ahead of print. PMID: 34038589 ***Co-corresponding author.*** Acknowledgement of federal support – YES

18. Sanders BE, Ku L, Walker P, **Bitler BG**. (2021). Assessing somatic mutations in matched biocompartments from patients with serous ovarian cancer: making sense of a heterogeneous pathology. *Technology in Cancer*. Jan-Dec 2021;20:15330338211027917. doi: 10.1177/15330338211027917. PMID: 34169762. Acknowledgement of federal support – YES

19. Clauset A, Behbakht K, and **Bitler BG** (2021). Decoding the dynamic tumor microenvironment. *Science Advances*. 04 Jun 2021: Vol. 7, no. 23, eabi5904 DOI: 10.1126/sciadv.abi5904. PMID: 34088677

20. Cari EL, Hagen-Lillevik S, Giornazi A, Post MD, Appiah L, **Bitler BG**, Polotsky AJ, Santoro N, Kieft J, Lai K, and Johnson J. (2021) Integrated Stress Response Control of Granulosa Cell Proliferation and Translation During Normal Ovarian Follicle Development. *Molecular Human Reproduction. ul 26;gaab050.* DOI: 10.1093/molehr/gaab050. PMID: 34314477

21. Steinhart B, Jordan KR, Bapat J, Post MD, Brubaker LJ, **Bitler BG***, and Wrobel J*. (2021) B Cell (CD19+) and Macrophage (CD68+) Spatial Interaction in the Tumor Microenvironment Associated with Higher Survival Probability. ePub Oct. 6th. *Molecular Cancer Research*. ***Co-corresponding author*** Acknowledgement of federal support – YES

22. Lin J, Guo D, Liu H, Zhou W, Wang C, Müller I, Kossenkov A, Drapkin R, **Bitler BG**, Helin K, and Zhang R. (2021). SETDB1-TRIM28 complex suppresses antitumor immunity. In press at *Cancer Research Immunology*.

23. Sanders BE, McMellen A, Yamamoto TM, Woodruff E, Post MD, and **Bitler BG**. (2021) DUSP1 inhibition in the treatment of high grade serous ovarian carcinoma. In review at *Molecular Cancer Therapeutics*. Acknowledgement of federal support – YES

24. Yamamoto TM, Webb PG, Baumgartner HK, Neville M, Behbakht K, **Bitler BG**. (2021). Loss of Claudin-4 reduces DNA damage repair and increase sensitivity to PARP inhibitors. In review at *Molecular Cancer Therapeutics*. Acknowledgement of federal support – YES

- **Books or other non-periodical, one-time publications.**
    - *Nothing to Report*
- **Other publications, conference papers, and presentations.** *Identify any other publications, conference papers and/or presentations not reported above. Specify the status of the publication as*

noted above. List presentations made during the last year (international, national, local societies, military meetings, etc.). Use an asterisk (*) if presentation produced a manuscript.

- Poster Presentation. DNA damage and claudin-4 expression. AACR Ovarian Cancer Focus. September 2018.
- Oral Presentation. Targeting Claudin-4 in combination with PARP inhibitors. Ovarian Cancer Midwest Focus Meeting. November 11-12th, 2021.
- Abstract Submitted. Targeting Claudin-4 in combination with PARP inhibitors. Society of Gynecologic Oncology. March, 2022.

- **Website(s) or other Internet site(s)**
  Nothing to Report
- **Technologies or techniques**
  Nothing to Report
- **Inventions, patent applications, and/or licenses**
  Nothing to Report
- **Other Products**
  Nothing to Report

PARTICIPANTS & OTHER COLLABORATING ORGANIZATIONS

- **What individuals have worked on the project?**

Name:	*Benjamin G. Bitler*
Project Role:	*Principal Investigator*
Researcher Identifier (e.g. ORCID ID):	*0000-0002-5809-5271*
Nearest person month worked:	*2*
Contribution to Project:	Directly oversees all aspects of the projects including data collection, analysis, and interpretation. Preparation and maintenance e of regulatory compliance.
Funding Support:	*DoD Pilot Award, The University of Colorado Start-up package, The American Cancer Society*

Name:	*Tomomi Yamamoto*
Project Role:	*Co-investigator*
Researcher Identifier (e.g. ORCID ID):	
Nearest person month worked:	*6*
Contribution to Project:	Data acquisition and interpretation. Day-to-day aspects of project
Funding Support:	*DoD Pilot Award* *American Cancer Society*

- *1)*
  - **Has there been a change in the active other support of the PD/PI(s) or senior/key personnel since the last reporting period?**

- *Yes, since the last reporting period the following new support has been obtained:*

Ovarian Cancer Research Program Department of Defense (Teal Expansion) 07/2021-6/2024
Grant Title: Investigating Combinatorial Approaches to Enhance cGAS/STING Activation and Anti-Tumor Immunity
Role: Principal Investigator
Total Cost:

Ovarian Cancer Research Program Department of Defense (Pilot Award) 07/2021-6/2023
Grant Title: Targeting the Oncogenic Protein Tyrosine Phosphatase PRL-3 with VDX-111 to Inhibit Ovarian Cancer
Role: Principal Investigator
Total Cost:

NIH/NCI R01CA261987 07/2021-6/2026
Grant Title: Targeting Wnt signaling in therapy-resistant ovarian cancer
Role: Principal Investigator
Total Cost:

SPECIAL REPORTING REQUIREMENTS

- *Nothing to Report*

APPENDICES:

- Yamamoto TM, Webb PG, Baumgartner HK, Neville M, Behbakht K, **Bitler BG**. (2021). Loss of Claudin-4 reduces DNA damage repair and increase sensitivity to PARP inhibitors. In review at *Molecular Cancer Therapeutics*. This manuscript represents the combined work of the DOD OCRP Pilot Award.

REFERENCES:

1. Cazzalini, O., A.I. Scovassi, M. Savio, L.A. Stivala, and E. Prosperi, *Multiple roles of the cell cycle inhibitor p21(CDKN1A) in the DNA damage response.* Mutat Res, 2010. **704**(1-3): p. 12-20. PMID: 20096807
2. Jazayeri, A., J. Falck, C. Lukas, J. Bartek, G.C. Smith, J. Lukas, and S.P. Jackson, *ATM- and cell cycle-dependent regulation of ATR in response to DNA double-strand breaks.* Nat Cell Biol, 2006. **8**(1): p. 37-45. PMID: 16327781
3. Osborn, A.J., S.J. Elledge, and L. Zou, *Checking on the fork: the DNA-replication stress-response pathway.* Trends Cell Biol, 2002. **12**(11): p. 509-16. PMID: 12446112
4. Zhou, B.B. and S.J. Elledge, *The DNA damage response: putting checkpoints in perspective.* Nature, 2000. **408**(6811): p. 433-9. PMID: 11100718
5. Hicks, D.A., C.E. Galimanis, P.G. Webb, M.A. Spillman, K. Behbakht, M.C. Neville, and H.K. Baumgartner, *Claudin-4 activity in ovarian tumor cell apoptosis resistance and migration.* BMC Cancer, 2016. **16**(1): p. 788. PMID: 27724921

Loss of Claudin-4 reduces DNA damage repair and increases sensitivity to PARP inhibitors

Tomomi M Yamamoto[1#], Patricia G. Webb[1#], Dana Davis[1], Heidi K. Baumgartner[1], Elizabeth Woodruff[1], Saketh R Guntupalli[2], Margaret Neville[1], Kian Behbakht[1,2], Benjamin G. Bitler[1]

[1]Divisions of Reproductive Sciences and [2]Gynecologic Oncology, Department of Obstetrics and Gynecology, University of Colorado Denver, Anschutz Medical Campus, 12700 E. 19th Avenue, Aurora, Colorado, 80045 USA

[#]co-first authors

Corresponding Author:

Benjamin Bitler, Ph.D.
Assistant Professor, Department of Obstetrics and Gynecology
Division of Reproductive Sciences
University of Colorado Denver Anschutz Medical Campus
Mail Stop 8613
12700 E. 19th Ave.
Aurora, CO 80045
Email: Benjamin.bitler@cuanschutz.edu

Fax: 303-724-3512

Authors declare no conflicts of interests.

ABSTRACT

High-grade serous ovarian cancer is the deadliest gynecologic malignancy due to the development of resistant disease. Claudin-4 is classically defined as a tight junction protein and is associated with female cancers. Claudin-4 is aberrantly expressed in nearly 70% of all ovarian cancer tumors and conveys a worse overall prognosis. Elevated claudin-4 expression correlates to increased DNA repair activity and resistance to DNA damaging agents. Poly(ADP) polymerase (PARP) inhibitors are emerging as an effective therapeutic option for patients with ovarian cancer and function by promoting DNA damage. The study examines the relationship between claudin-4 expression and response to PARP inhibitors. The study uses both genetic and pharmacologic inhibition of claudin-4 in in vitro and ex vivo models of ovarian cancer to examine DNA repair markers and functional activity. Genetic inhibition of claudin-4 results in the downregulation of several DNA damage repair effectors, including 53BP1 and XRCC1. Also, claudin-4 knockdown does not change homology-directed repair but inhibits non-homologous end-joining and reduces 53BP1 foci formation. In 15 primary ovarian cancer tumors, higher claudin-4 expression significantly correlated to a dampened PARP inhibitor-mediated anti-proliferation response. Further, claudin-4 inhibition in high claudin-4 tumors sensitized tumor sections to PARP inhibition. These data highlight that claudin-4 expression in ovarian cancer tumors could potentially serve as both a marker of PARP inhibitor response and a therapeutic target to improve PARP inhibitor response.

INTRODUCTION

High grade serous ovarian carcinoma (HGSOC) is the most common epithelial derived ovarian cancer and is the deadliest. Several factors contribute to HGSOC-related deaths including inadequate early detection, diagnosis at advanced stage disease, and the development of acquired therapy resistance. In the last six years, the development of poly(ADP) ribose polymerase (PARP) inhibitors (PARPi) has led to a significant shift in the clinical care of patients with ovarian cancer.

PARPi exploit deficiencies in DNA damage repair pathways. Approximately, 50% of ovarian cancers have some degree of Homologous Recombination (HR) DNA repair deficiency (HRD); these deficiencies are most common in tumors with mutations in BRCA1/2 [1]. BRCA1/2 proteins are directly involved in HR DNA repair and DNA damage repair capacity is an important biomarker of PARPi responsiveness. PARPi prevent single-strand DNA break repair and in the context of HR repair deficiencies, PARPi facilitate the accumulation of replication induced DNA double strand breaks (DSBs). These effects culminate in catastrophic mitotic failure and cell death. Clinical trials for olaparib and niraparib have demonstrated that the PARPi response can occur in tumors without mutations in *BRCA1/2* genes [2, 3]. For instance, niraparib significantly extended progression-free survival in patients without germline BRCA1/2 mutations compared to placebo, 9.3 versus 3.9 months, respectively (hazard ratio, 0.45; 95% confidence interval, 0.34 to 0.61) [4]. In HGSOC patients, the major clinical challenges in the use of PARPi include: (1) identification of patients likely to respond, (2) sensitizing non-BRCA1/2 mutated HGSOC tumors to PARPi, and (3) addressing resistance to PARPi.

Claudin-4 (*CLDN4*) is expressed in approximately 70% of all human HGSOC tumors. It is highly expressed in ovarian tumor cells that: 1) are more resistant to cisplatin/carboplatin and paclitaxel [5, 6] 2) have increased migratory potential [7, 8] and 3) display stem-like properties [6, 9]. Previously, we reported that the loss of claudin-4 expression led to aberrant cell cycle progression and G2/M arrest [10]. We previously designed a small claudin mimic peptide (CMP)

that interferes with the DFYNP sequence in the second extracellular loop of claudin-4 [11]. CMP is used in the D-amino acid conformation to increase peptide stability. The peptide disrupts claudin-4 activity; further CMP increased tumor cell response to a potent apoptotic inducer, staurosporine, and inhibited tumor cell migration [7].

Patients with HGSOC tumors expressing claudin-4 protein have poorer survival compared to patients with tumors lacking claudin-4 [12]. Analyses of HGSOC tumors in The Cancer Genome Atlas (TCGA) revealed a tendency toward mutual exclusion of *CLDN4* amplification/overexpression and *BRCA1/2* mutation/downregulation [1], suggesting that claudin-4 may serve as potential marker of PARP inhibitor response. Notably, in breast cancer, the "claudin-low" subtype is often more responsive to PARP inhibitors [13]. For this reason, we have assessed the role of claudin-4 in PARP inhibitor response in models of HGSOC.

In particular, here we have extended our previous claudin-4 experiments to examine its effect on the PARPi response as well as to define claudin-4-mediated mechanisms of DNA repair. We discovered that in HGSOC cells without BRCA-mutations or HRD loss that knocking down claudin-4 expression increased PARPi sensitivity. Comparing the transcriptome of claudin-4 high and low expressing tumors, in claudin-4 high tumors we found enrichments for DNA repair, DNA replication, and cell cycle regulatory pathways. Examination of Dependency Mapping [14] across multiple cancer types revealed that increased *CLDN4* expression correlated with a blunted response to three different PARPi (olaparib, rucaparib, niraparib). Examining a reverse phase protein array of claudin-4 knockdown HGSOC cells, we observed significant down regulation of several DNA repair proteins (e.g., XRCC1 and 53BP1). Further, claudin-4 knockdown did not inhibit HR repair, but did significantly attenuate non-homologous end joining (NHEJ) DNA repair. In *ex vivo* models of primary ovarian cancer tumors, combined claudin-4 inhibition via CMP and PARP inhibition promoted an anti-proliferation and apoptotic response. Thus, targeting claudin-4 expression in combination with PARPi in HGSOC tumors represents a novel therapeutic strategy.

METHODS

Cell culture: Human-derived OVCAR3, OVCAR4, OVCAR8, OVCAR10, and OVCA429 were obtained from The Gynecologic Tumor and Fluid Bank at the University of Colorado. Cells were cultured in RPMI-1640 medium (Gibco, Thermo Fisher Scientific, Grand Island, NY, USA) plus 10% heat-inactivated fetal bovine serum (Access Cell Culture, Vista, CA, USA) and 1% penicillin/streptomycin (Gibco, Thermo Fisher Scientific) at 37°C and 5% CO_2. 293FT cells were obtained by the University of Colorado Functional Genomic shared resource. All cell lines were authenticated at the beginning of this study by short tandem repeat profiling at the University of Arizona. Cells are monthly tested for mycoplasma (LookOut, Sigma # MP0035-1KT) and were tested as recently as July 20th, 2021.

Immunoblot analysis: To analyze levels of claudin-4 protein expression, tumor cells were scraped from culture plates in the presence of lysis buffer (30 mM Tris HCl pH7.4, 150 mM NaCl, 1% TritonX-100, 10% glycerol, 2 mM EDTA, 0.57 mM PMSF, 1X cOmplete^{TM} Protease Inhibitor Cocktail), placed on a shaker for 10 minutes and spun at 13,000 rpm for 10 minutes. Protein was separated by SDS-PAGE and transferred to PVDF membrane using the TransBlot Turbo (BioRad). Membranes were blocked with Intercept Blocking Buffer (LI-COR, #927-60001) for 1 hour at room temperature. Mouse anti-human claudin-4 (ThermoFisher #32-9400, 1:500),, rabbit anti-human β-actin (1:10,000; Abcam, Cambridge, MA, USA), or mouse anti-GAPDH (1:2500, Invitrogen, #MA5-15738) primary antibody incubation was performed overnight at 4 °C. Membranes were washed 3 times for 5 minutes each in TBST (50 mM Tris pH 7.5, 150 mM NaCl, 0.1% Tween-20), followed by secondary antibodies for one hour at room temperature. Membranes were washed again 3 times for 5 minutes each in TBST. For fluorescent detection, bands were visualized using the LI-COR Odyssey Imaging System.

Reverse-transcriptase quantitative PCR (RT-qPCR): RNA was isolated from cells using the RNeasy Plus Mini Kit (Qiagen). mRNA expression was determined using SYBR green Luna One Step RT-qPCR Kit (New England BioLabs) on a C1000 Touch (Bio-Rad) or QuantStudio 6 (Applied Biosystems) thermocycler. Expression was quantified by the ΔΔCt method using target-specific and control primers. β-2-microglobulin (*B2M*) used as an internal control. Primer sequences: *B2M* Fwd 5'-GGCATTCCTGAAGCTGACA-3, Rev 5'-CTTCAATGTCGGATGGATGAAAC-3', *CLDN4* Fwd 5'-GCCTTACTCCGCCAAGTATT-3', Rev 5- AGGGAAGAACAAAGCAGAGAG-3' [15].

Immunofluorescence: After treatment, cells were washed with phosphate buffered saline (PBS; Gibco, Thermo Fisher Scientific) and fixed with 10% phosphate buffered formalin (Fisher Scientific, Pittsburg, PA, USA) at room temperature (RT) for 15 minutes. Cells were washed twice with PBS before cell membrane permeabilization with 0.5% Triton X-100 (IBI Scientific, Peosta, IA, USA) for 5 minutes and washed again with PBS. Cells were treated with blocking buffer (2% bovine serum albumin; Sigma-Aldrich) for 1 hour before application of primary antibody to claudin-4 (ThermoFisher #32-9400, 1:100), XRCC1 (Cell Signaling #2735, 1:100) 53BP1 (Cell Signaling #4937, 1:100) and γH2ax (EMDMillipore #05-636, 1:400) overnight at 4°C. Cells were then washed with PBS five times before application of secondary antibody Alexa Fluor 488-conjugated donkey anti-mouse secondary antibody (Invitrogen #A21202, 1:1000) or CY3 conjugated donkey anti-rabbit secondary antibody (1:100; Jackson ImmunoResearch Laboratories, West Grove, PA, USA); 5 μg/ml 4',6-diamidina-2-phenylindole (DAPI; Sigma) was applied for 45 minutes at room temperature followed by five washings with PBS. After removal of PBS, o-phenylenediamine dihydrochloride (20 mg/ml; OPDA) in 1M Tris, pH 8.5 was added to the slides to preserve fluorescence and coverslip mounted. Imaging was performed in the Advanced Light Microscopy Core in the NeuroTechnology Center at University of Colorado Anschutz Medical Campus using the 3I Marianas inverted spinning disk confocal

microscope. Images were analyzed using SlideBook software (Intelligent Imaging Innovations, Inc., Denver, CO, USA) [10].

Lentiviral shRNA knockdown: Lentiviral knockdown was completed as described [10]. Briefly, lentivirus was packaged as previously described in [16]. Using 293FT cells using 3rd generation packaging plasmids (Virapower, Invitrogen) with polyethyleneimene (PEI) transfection in a 1:3 DNA:PEI ratio. Culture supernatant was harvested at 48-72 h post-transfection and processed through 0.45 μM filters. Viruses encoded a puromycin resistance gene. Transduced OVCAR3 and OVCA429 cells were selected in 1 μg/mL puromycin. Claudin-4 shRNA (TRC#: TRCN0000116627 or TRCN0000116628) or control shRNA (SHC001, pLK0.1-puro Empty Vector) lentiviral suspension (Sigma-Aldrich MISSION® shRNA, University of Colorado Functional Genomics Facility, Aurora, CO, USA) was added to the cells and incubated overnight at 37°C. Fresh medium was added to remove lentivirus and cells were allowed to recover for 24 hours before being treated with 0.5 μg/ml puromycin for selection and expansion of transduced cells. Western blot analysis was performed to confirm loss of claudin-4 expression.

Colony formation assay: As previously described in [15]. Olaparib (#S1060) and Rucaparib (#S4948) were obtained from SelleckChem. Cell lines were seeded in 24-well plates and treated with increasing doses of olaparib. Media and PARP inhibitor were changed every three days for 12 days or until control wells were confluent, whichever occurred first. Colonies were washed twice with PBS, then incubated in fixative (10% methanol/10% acetic acid in PBS). Fixed colonies were stained with 0.4% crystal violet in PBS. After imaging, crystal violet was dissolved in fixative and absorbance was measured at 570 nm using a Molecular Devices SpectraMax M2e plate reader.

Ovarian cancer dataset analysis: Publicly available cancer databases: Ovarian cancer single cell RNA-sequencing [17] accessed April 9th, 2021 via http://blueprint.lambrechtslab.org/; Claudin-4 expression correlation with cisplatin, olaparib, rucaparib, and niraparib sensitivity was accessed on March 22nd 2021 via https://depmap.org/portal/ [14, 18]. Claudin-4 low and high (based on median RNA expression) RNA-sequencing and mutational count analyses from The Cancer Genome Atlas Ovarian Serous Cystadenocarcinoma Firehose Legacy accessed on Dec. 20th 2020 via https://cbioportal.org [1, 19, 20].

Two-plasmid functional DNA repair assay: Two-plasmid functional assays were performed to assess distal non-homologous end joining (NHEJ) and homology directed repair (HDR) [21]. Cells were transfected with pimEJ5GFP (NHEJ) or pDRGFP (HDR). Cells were transfected with I-SceI, which introduces DNA double-strand breaks in the plasmids. After 72 hours, cells were collected and examined via a flow cytometer to quantify GFP positive cells. pimEJ5GFP was a gift from Jeremy Stark (Addgene # 44026). pDRGFP and pCBASceI were gifts from Maria Jasin (Addgene # 26475/26477).

Immunofluorescence: Cells grown on Type I collagen (Sigma) coated glass slides were fixed with 10% phosphate buffered formalin (Sigma) at room temperature (RT) for 15 min. Cells were washed twice with phosphate buffered saline (PBS), permeabilized with 0.5% Triton X-100 (Sigma) for 5 minutes at RT, washed twice with PBS, and blocked with 2% bovine serum albumin (Sigma) for 1 hour at RT before application of primary antibody to claudin-4 (ThermoFisher #32-9400, 1:100), XRCC1 (Cell Signaling #2735, 1:100), 53BP1 (Cell Signaling #4937, 1:100) and yH2ax (EMDMillipore #05-636, 1:400) overnight at 4°C. Cells were washed with PBS five times before application of secondary antibodies conjugated to a fluorescent probe (1:100, Jackson ImmunoResearch) and 5 µg/ml 4',6-diamidina-2-phenylindole (DAPI,

Sigma) for 45 minutes at RT followed by five washes with PBS. OPDA (20 mg/ml, o-phenylenediamine dihydrochloride (Sigma) in 1M Tris, pH 8.5 and 10% glycerol was applied to slides for preservation of fluorescence and coverslip mounted. Imaging was performed in the Advanced Light Microscopy Core part of NeuroTechnology Center at University of Colorado Anschutz Medical Campus using the 3I Marianas inverted spinning disk confocal microscope. Images were analyzed using SlideBook software (Intelligent Imaging Innovations Inc., Denver, CO, USA).

Ex vivo culture. Primary ovarian cancer tumor samples were obtained from the Gynecologic and Tumor Fluid Bank at the University of Colorado (COMIRB #07-935). Tumors were sectioned at 300 micron thickness using a Krumdieck Tissue Slicer. Claudin-mimetic peptide CMP (NH2-GDGYNPG-OH, D-amino acid conformation) was obtained from the University of Colorado Protein and Peptide Chemistry Core [11]. Tumor sections were cultured with vehicle control, olaparib (1 μM), CMP (400 μM) or in combination olaparib/CMP (1 μM/400 μM, respectively) for 72 hours. Following a 72-hour incubation, tissue sections were fixed in 10% buffered formalin, paraffin embedded and sectioned. Tumor sections were analyzed by immunohistochemistry.

Immunohistochemistry: Paraffin embedded sections were dewaxed in xylene twice for 5 min and rehydrated in graded alcohols at 100%, 90%, 70%, and 30% for 3 min each and then in PBS for 5 min. Antigen retrieval was performed using Antigen Unmasking Solution #H-3300, Vector Laboratories, Burlingame, CA, placing the slides in the solution for 10 rounds of heating to boiling for 10 seconds followed by cooling for 45 seconds. Sections were treated with 0.2% glycine in PBS for 30 min, rinsed twice with PBS, and then blocked with 10% normal donkey serum and 0.1 mg/ml saponin in PBS for 60 min. Sections were incubated at 4 C overnight with

antibody to claudin-4 (ThermoFisher #32-9400, 1:100). Sections were rinsed five times in PBS and then incubated with Alexa Fluor 488 conjugated donkey anti mouse secondary antibody (Jackson Immunoresearch #715-545-150, 1:100) and 5 µg/ml 4',6-diamidina-2-phenylindole (DAPI, Sigma) for 45 minutes at RT followed by five washes with PBS. OPDA (20 mg/ml, o-phenylenediamine dihydrochloride (Sigma) in 1M Tris, pH 8.5 and 10% glycerol) was applied to slides for preservation of fluorescence and coverslip mounted. Ki67 (Thermo Scientific, cat. # RM-9106) and cleaved caspase 3 (Cell Signaling, cat. # 9661) were completed by the Histopathology Shared Resource as described in [22]. Tumor sections were also stained for the Mullerïan marker, PAX8 (Proteintech #10336-1-AP 1:100). Treatment groups were de-identified and an H-scores were calculated for each tumor section as previously described [23]. Imaging was performed in the Advanced Light Microscopy Core part of NeuroTechnology Center at University of Colorado Anschutz Medical Campus using the 3I Marianas inverted spinning disk confocal microscope. Images were analyzed using SlideBook software (Intelligent Imaging Innovations Inc., Denver, CO, USA)

Statistics: Graphs and statistical analysis were completed in Prism GraphPad (v9). Data are presented as mean ± standard error of the mean (s.e.m.). An unpaired Student *t* test was used for statistical comparison between control and treatment groups. Dose response curves were calculated using non-linear regression via the log(inhibitor) vs. response equation. A one-way ANOVA was used to determine variance among multiple gestational groups, with a Benjamini-Hochberg Multiple Comparison post-test to determine significance between individual groups. A p value of < 0.05 was considered significant.

RESULTS

Claudin-4 expression is correlated with cell cycle regulation and DNA repair in high grade serous epithelial ovarian tumors. Based on the combined molecular score of claudin-4/*CLDN4* across a variety of epithelial cancers, the molecule is often associated with female cancers, specifically ovarian cancer (Figure S1A). Further, elevated claudin-4 expression portends poor prognosis in three of six primary ovarian cancer tumor datasets (Figure S1B). For this reason, to begin to identify the role of claudin-4 in HGSOC tumors, TCGA tumors were stratified to "high" or "low" claudin-4 expression based on median expression (Figure 1A). Comparing the transcriptome of the tumors based on claudin-4 expression we identified 1,582 differentially expressed transcripts (FDR<0.05, Figure 1B and Table S1). Comparing these 1,582 genes to the Reactome [24] gene sets, there was a significant enrichment of genes involved in cell cycle, DNA repair and DNA replication pathways (Red dots, Figure 1C), including RNA Polymerase II Subunit J (*POLR2J*), BRCA1 Interacting Protein C-Terminal Helicase 1 (*BRIP1*), Nucleoporin 160 (*NUP160*) and Protein Kinase, DNA-Activated, Catalytic Subunit (*PRKDC*) (Figure 1D). These data are consistent with previous reports that loss of claudin-4 expression promotes cell cycle arrest [10]; however, a claudin-4 connection to DNA damage response had not been established.

DNA damaging agents are standard of care treatments for HGSOC, including platinum--based chemotherapies and Poly(ADP) Ribose Polymerase inhibitors (PARPi). Using Dependency Mapping (DepMap) [18], we examined the correlations of claudin-4 mRNA expression with sensitivity to cisplatin and three FDA-approved PARPi: olaparib, rucaparib, and niraparib. Examining over 400 different cell lines, there was a significant positive correlation between claudin-4 mRNA expression and decreased sensitivity (Area under the curve, AUC) to cisplatin, olaparib, niraparib, and rucaparib (Figure 1E). Specifically, the higher expression of claudin-4 mRNA significantly correlated to drug sensitivity AUC. Thus, cells with low claudin-4

expression have increased sensitivity to DNA damaging agents. These data are consistent with the TCGA RNA-seq analysis and suggest a novel and previously undefined claudin-4/DNA repair axis.

Loss of claudin-4 expression increases sensitivity to PARPi

To more directly establish the role of claudin-4 in conveying sensitivity to anti-cancer therapies we examined claudin-4 protein expression in 13 HGSOC cell lines (Figure 2A and S2A). We detailed the BRCA-status of each of the cell lines (Table S2). Appreciating a need to improve options for patients without BRCA-mutations the cell lines examined are BRCA1/2-wildtype, essential in considering sensitivity to PARPi. In the four HGSOC cell lines shown in Fig 2A, we measured PARPi sensitivity using either olaparib or rucaparib (Figure 2B-E and S2B). We observed that the 50% inhibitory concentration (IC50) of olaparib did not correlate with claudin-4 expression. In contrast, the IC50 of rucaparib aligned with the DepMap data showing the lower claudin-4 expressing cells had increased sensitivity. As nearly 70% of HGSOC tumors express claudin-4, we next wanted to determine if loss of claudin-4 expression improved response to PARPi. Using a control shRNA or two independent small-hairpin RNAs (shRNA) specific for *CLDN4,* we knocked down both claudin-4 mRNA and protein expression in both OVCAR3 and OVCA429 cell lines (Figure 2F and S2C). Next, the shControl and claudin-4 knockdown cells were examined for olaparib and rucaparib response. The loss of claudin-4 significantly reduced the IC50 of both olaparib and rucaparib compared to the shControl cells (Figure 2G-H and S2D-E). As olaparib is more widely used compared to rucaparib, we used olaparib for the remaining experiments. These data directly demonstrate that reducing claudin-4 expression increases sensitivity to PARPi.

Mechanism by which loss of Claudin-4 expression increases sensitivity to PARPi

To define the mechanism of claudin-4 mediated PARPi response, we examined via RPPA the signaling pathways effected by claudin-4 downregulation. Using the OVCAR3 shControl compared to the shCLDN4 cells, we observed differential expression of multiple proteins encompassing the pathways, DNA damage response, receptor tyrosine kinase signaling, and transcription factor expression (Figure 3A). Specifically, we observed loss of claudin-4 with two different shRNA constructs significantly reduced the protein expression of XRCC1 and 53BP1 (Figure 3B-C). X-Ray Repair Cross Complementing 1 (XRCC1) directly interacts with PARP to promote single-strand DNA damage repair and XRCC1 knockdown increases sensitivity to olaparib [25]. Tumor Protein P53 Binding Protein (*TP53BP1*/53BP1) is recruited to site of DNA damage via histone modifications (e.g., phosphorylation, methylation, ubiquitination) and promotes non-homologous end-joining (NHEJ) and antagonizes HR repair. Using the DepMap database of ovarian cancer cells line, while claudin-4 mRNA expression did not correlate with 53BP1 protein expression in HGSOC cell lines, it did with XRCC1 protein expression (Figure 3D-E). Interestingly, using untargeted mass spectrometry data in 12 ovarian cancer [26], we examined the correlation between claudin-4 and XRCC1 or 53BP1 protein expression, there was only a positive correlation between claudin-4 and 53BP1 (Figure S3A-B). Consistently, we performed an unbiased screen of 126 FDA approved anti-cancer therapies (NCI Approved Oncology Drug Panel). In shCLND4 compared to shCtrl cells, most of the agents that demonstrated increased sensitivity in shCLND4 cells were DNA damaging agents measured by colony formation (Figure 3F). These findings are consistent with previous reports demonstrating claudin-4 correlates to DNA damaging agent resistance such as cisplatin [12] and paclitaxel [10]. However, little is known regarding claudin-4 and the response to PARPi, although they are currently approved for the HGSOC upfront maintenance therapy. Single-cell sequencing of HGSOC tumors [17] showed that claudin-4, *TP53BP1*, and *XRCC1* expression were largely restricted to PAX8-positive tumor cells (Figure 3G), highlighting that loss of claudin-4 would likely impact the DNA repair capacity of the tumor compartment. While there is

variability between the claudin-4 knockdown, these data demonstrate that modulation of claudin-4 expression in tumor cells is correlated to DNA damage response effectors, including XRCC1 and 53BP1.

Loss of claudin-4 attenuates XRCC1and 53BP1 foci formation and blunts the DNA damage repair response

Knockdown of claudin-4 resulted in the downregulation of DNA repair effectors, including 53BP1 and XRCC1. Thus, using the I-SceI-based functional DNA repair assays [21] we measured the DNA repair activity in cells that have claudin-4 knocked down. While shCLDN4#1 did not show altered homology-directed DNA repair compared to shCtrl, shCLDN4#2 did reduce repair activity, although not significantly (Figure 4A). In contrast, in both shCLDN4 #1 and #2 cells we observed a significant 2-fold decrease in GFP positive cells following DNA damage induction via I-SceI transfection indicating that loss of claudin-4 inhibited canonical NHEJ-mediated DNA repair (Figure 4B). This finding is consistent with the loss of 53BP1 expression in claudin-4 knockdown cells.

To confirm that the loss of claudin-4 blunted 53BP1 and NHEJ DNA damage repair, we next used immunofluorescence to evaluate XRCC1, 53BP1, and γH2ax foci formation in claudin-4 knockdown HGSOC cells following PARPi treatment. Consistent with the RPPA data we observed a decrease in XRCC1 protein expression (Figure 4C). Olaparib treatment induced variable γH2ax foci formation in shCtrl and shCLDN4 cells (Figure 4C). Consistent with the functional DNA repair assays, olaparib induced 53BP1 foci formation in shCtrl cells, but 53BP1 foci formation was significantly blunted following claudin-4 knockdown (Figure 4D-E), suggesting a decrease in NHEJ DNA repair. These data clearly demonstrate a relationship between claudin-4 expression and DNA repair capacity. To further establish this relationship, we examined mutational burden in ovarian cancer tumors. In ovarian cancer tumors profiled in

TCGA, lower claudin-4 mRNA and protein expression significantly correlated to elevated mutational burden (Figure 4F). These data suggest that down regulation of claudin-4 directly inhibits DNA repair and claudin-4 loss appears to be more detrimental to NHEJ activity.

Treating ovarian cancer tumors in combination with claudin-4 inhibitory peptide and olaparib

We next assessed the apoptotic and proliferation capacity of primary ovarian cancer tumors treated with CMP and/or olaparib. Primary ovarian cancer tumors were uniformly sectioned and treated for 72 hrs (Figure 5A). Tumor sections were analyzed for Ki67 (proliferation), cleaved caspase 3 (CC3), claudin-4, and PAX8. Through the collaboration with the Gynecologic Tumor and Fluid Bank, we sectioned and examined the response of CMP and/or olaparib in 15 primary ovarian cancer tumors (10 HGSOC, 2 high grade carcinosarcoma [HGCS], 1 low grade SOC, 1 mucinous, and 1 granulosa cell tumor) (Table S3). In the non-HGSOC tumors, we observed a varied effect of CMP and olaparib treatment on proliferation and apoptosis (Figure S4A). Expression of the Mullerïan marker PAX8 express was completed to ensure histological analysis within the HGSOC tumor compartments (Figure S4B). In the HGSOC tumors, we observed three HRD positive, one HRD negative and eight HRD unknown tumors. There were six BRCA-wildtype and six tumors with unknown BRCA-status (Table S3). In the serous and carcinosarcoma tumors, we determined claudin-4 expression via immunofluorescence (Figure 5B-C and S4B). We noted varied apoptotic effects within CMP, olaparib, and CMP/olaparib (Figure S4C-D). In contrast, within the HGSOC tumors, we consistently observed that olaparib and/or CMP significantly inhibited proliferation as shown by a significant decrease in Ki67 (Figure 5B-D and S4E-F). Consistent with the *in vitro* data, claudin-4 null/low tumors had consistently and significantly lower Ki67 compared to control ($p<0.0001$). In contrast, claudin-4 high tumors exhibited a variable and non-significant anti-proliferative response to olaparib compared to the control tumors (Figure 5E). However,

CMP/olaparib combination significantly inhibited proliferation independent of claudin-4 expression, suggesting claudin-4 inhibition may be promoting a “BRCAness” state in improving olaparib response. These data generated from primary ovarian cancer tumors demonstrate that low claudin-4 expression correlates to olaparib sensitivity. Also, combining claudin-4 inhibition and olaparib is potentially a novel combinatory approach to treating patients that are insensitive to olaparib.

DISCUSSION

Beyond BRCA and HRD-status there are limited molecular markers that correspond to response to standard of care DNA damaging agents, such as platinum-based chemotherapies and PARP inhibitors. Claudin-4 is classically depicted as a tight junction protein, is expressed in 70% of all ovarian cancers, and may serve as additional predictive marker in therapeutic response. In this report, we observed that lower claudin-4 expression correlated to improved response to DNA damaging agents, including PARP inhibitors. Also, knocking down claudin-4 decreased functional non-homologous mediated DNA repair activity and modulated the expression and foci formation capacity of DNA repair effectors. Notably, in a panel of primary ovarian cancer tumors, low claudin-4 expressing tumors had an improved anti-proliferative response to olaparib and in high claudin-4 expressing tumors the combination of claudin-4 inhibition and olaparib promoted a robust anti-proliferative response.

PARP inhibitors represent a breakthrough in cancer care and while initially approved for ovarian cancer, they are now FDA-approved for metastatic breast, pancreatic, and castration-resistant prostate cancer [27]. Germline BRCA-mutations and homologous recombination deficiency (HRD) status remain the most widely used molecular markers that predict PARP inhibitor response. However, there remains a paucity of targeted therapeutics for patients without BRCA-mutations and/or are HR proficient. For this reason, there is significant interest in promoting a “BRCAness” like state in HR proficient tumors to improve PARP inhibitor response. Knockdown of claudin-4 led to the downregulation of several DNA repair factors, including 53BP1 and XRCC1 and inhibition of NHEJ repair. Previous reports have shown 53BP1 loss leads to PARP inhibitor resistance, but the resistant phenotype was dependent on the status of BRCA and HRD [28, 29]. With respect to XRCC1, in an ovarian cancer model loss of XRCC1 induced a synthetic lethality with olaparib [30]. While we report here a direct link between loss of claudin-4 expression and DNA damage repair activity, there is evidence of this link within the

ovarian cancer TCGA dataset: low expressing claudin-4 tumors more often have an elevated mutational count. These studies suggest that a claudin-4 mediated decrease of both XRCC1 and 53BP1 could be promoting DNA repair-deficiency or BRCAness, enhancing the response to DNA damaging agents.

Leveraging *ex vivo* culture of primary human ovarian cancer tumors we demonstrated that tumors with high claudin-4 were more resistant to olaparib compared to tumors with low claudin-4. Excitingly, while we the number of tumors examined was limiting, claudin-4 inhibition via CMP in ovarian cancer tumors with high claudin-4 increased the sensitivity to olaparib. Several studies have suggested the potential of targeting claudin-4 to inhibit ovarian cancer progression [7, 10, 31], and while CMP has both *in vitro* and *in vivo* efficacy [7, 10] the necessary dose is not physiologically possible. Claudin-4 expression is mainly confined to transformed epithelial cells [10, 31]; it therefore offers a targeted approach to inhibiting cancer progression with minimal off-target effects. Thus, future work will investigate combining CMP's claudin-4-specificity [7, 11] with the targeted protein degrader technology, proteolysis-targeting chimeras (PROTAC).

In conclusion, claudin-4 expression is directly related to the DNA damage response and conveys decreased sensitivity to the standard of care for ovarian cancer, including PARP inhibitors. In the context of BRCA-wildtype and HR-proficient ovarian cancer, claudin-4 expression may serve as predictor of therapeutic response and offer a molecular marker-based rationale for combining claudin-4 inhibition with DNA damaging agents.

ACKNOWLEDGEMENTS

We acknowledge philanthropic contributions from Kay L. Dunton Endowed Memorial Professorship In Ovarian Cancer Research, the McClintock-Addlesperger Family, Karen M. Jennison, Don and Arlene Mohler Johnson Family, Michael Intagliata, Duane and Denise Suess, Mary Normandin, and Donald Engelstad. This work was supported by The Department of Defense (Bitler, OC170228, OC200302, OC200225), The American Cancer Society (Bitler, RSG-19-129-01-DDC), and NIH/NCI (Bitler, R37CA261987). The RPPA Core at MD Anderson is supported by NCI Grant # CA16672 and Dr. Yiling Lu's NIH R50 Grant #R50CA221675: Functional Proteomics by Reverse Phase Protein Array in Cancer. Imaging supported in part by Rocky Mountain Neurological Disorders Core Grant Number P30 NS048154 and by Diabetes Research Center Grant Number P30 DK116073. The University of Colorado Cancer Center Support Grant (P30CA046934).

REFERENCES

1. *Integrated genomic analyses of ovarian carcinoma.* Nature, 2011. **474**(7353): p. 609-15. PMID: 21720365
2. Domchek, S.M., C. Aghajanian, R. Shapira-Frommer, R.K. Schmutzler, M.W. Audeh, M. Friedlander, J. Balmana, G. Mitchell, G. Fried, S.M. Stemmer, A. Hubert, O. Rosengarten, N. Loman, J.D. Robertson, H. Mann, and B. Kaufman, *Efficacy and safety of olaparib monotherapy in germline BRCA1/2 mutation carriers with advanced ovarian cancer and three or more lines of prior therapy.* Gynecol Oncol, 2016. **140**(2): p. 199-203. PMID: 26723501
3. Matulonis, U.A., R.T. Penson, S.M. Domchek, B. Kaufman, R. Shapira-Frommer, M.W. Audeh, S. Kaye, L.R. Molife, K.A. Gelmon, J.D. Robertson, H. Mann, T.W. Ho, and R.L. Coleman, *Olaparib monotherapy in patients with advanced relapsed ovarian cancer and a germline BRCA1/2 mutation: a multistudy analysis of response rates and safety.* Ann Oncol, 2016. **27**(6): p. 1013-9. PMID: 26961146
4. Mirza, M.R., B.J. Monk, J. Herrstedt, A.M. Oza, S. Mahner, A. Redondo, M. Fabbro, J.A. Ledermann, D. Lorusso, I. Vergote, N.E. Ben-Baruch, C. Marth, R. Madry, R.D. Christensen, J.S. Berek, A. Dorum, A.V. Tinker, A. du Bois, A. Gonzalez-Martin, P. Follana, B. Benigno, P. Rosenberg, L. Gilbert, B.J. Rimel, J. Buscema, J.P. Balser, S. Agarwal, U.A. Matulonis, and E.-O.N. Investigators, *Niraparib Maintenance Therapy in Platinum-Sensitive, Recurrent Ovarian Cancer.* N Engl J Med, 2016. **375**(22): p. 2154-2164. PMID: 27717299
5. Stewart, J.J., J.T. White, X. Yan, S. Collins, C.W. Drescher, N.D. Urban, L. Hood, and B. Lin, *Proteins associated with Cisplatin resistance in ovarian cancer cells identified by quantitative proteomic technology and integrated with mRNA expression levels.* Mol Cell Proteomics, 2006. **5**(3): p. 433-43. PMID: 16319398
6. Casagrande, F., E. Cocco, S. Bellone, C.E. Richter, M. Bellone, P. Todeschini, E. Siegel, J. Varughese, D. Arin-Silasi, M. Azodi, T.J. Rutherford, S. Pecorelli, P.E. Schwartz, and A.D. Santin, *Eradication of chemotherapy-resistant CD44+ human ovarian cancer stem cells in mice by intraperitoneal administration of clostridium perfringens enterotoxin.* Cancer, 2011. PMID: 21692061
7. Hicks, D.A., C.E. Galimanis, P.G. Webb, M.A. Spillman, K. Behbakht, M.C. Neville, and H.K. Baumgartner, *Claudin-4 activity in ovarian tumor cell apoptosis resistance and migration.* BMC Cancer, 2016. **16**(1): p. 788. PMID: 27724921
8. Yin, G., A.B. Alvero, V. Craveiro, J.C. Holmberg, H.H. Fu, M.K. Montagna, Y. Yang, I. Chefetz-Menaker, S. Nuti, M. Rossi, D.A. Silasi, T. Rutherford, and G. Mor, *Constitutive proteasomal degradation of TWIST-1 in epithelial-ovarian cancer stem cells impacts differentiation and metastatic potential.* Oncogene, 2013. **32**(1): p. 39-49. PMID: 22349827
9. Janzen, D.M., E. Tiourin, J.A. Salehi, D.Y. Paik, J. Lu, M. Pellegrini, and S. Memarzadeh, *An apoptosis-enhancing drug overcomes platinum resistance in a tumour-initiating subpopulation of ovarian cancer.* Nat Commun, 2015. **6**: p. 7956. PMID: 26234182
10. Breed, C., D.A. Hicks, P.G. Webb, C.E. Galimanis, B.G. Bitler, K. Behbakht, and H.K. Baumgartner, *Ovarian Tumor Cell Expression of Claudin-4 Reduces Apoptotic Response to Paclitaxel.* Mol Cancer Res, 2019. **17**(3): p. 741-750. PMID: 30606772
11. Baumgartner, H.K., N. Beeman, R.S. Hodges, and M.C. Neville, *A d-Peptide Analog of the Second Extracellular Loop of Claudin-3 and -4 Leads to MisLocalized Claudin and Cellular Apoptosis in Mammary Epithelial Cells.* Chem Biol Drug Des, 2011. **77**(2): p. 124-36. PMID: 21266016

12. Yoshida, H., T. Sumi, X. Zhi, T. Yasui, K. Honda, and O. Ishiko, *Claudin-4: a potential therapeutic target in chemotherapy-resistant ovarian cancer.* Anticancer Res. **31**(4): p. 1271-7. PMID: 21508375
13. Lehmann, B.D., J.A. Bauer, X. Chen, M.E. Sanders, A.B. Chakravarthy, Y. Shyr, and J.A. Pietenpol, *Identification of human triple-negative breast cancer subtypes and preclinical models for selection of targeted therapies.* J Clin Invest, 2011. **121**(7): p. 2750-67. PMID: 21633166
14. Vazquez, F. and J.S. Boehm, *The Cancer Dependency Map enables drug mechanism-of-action investigations.* Mol Syst Biol, 2020. **16**(7): p. e9757. PMID: 32696566
15. Watson, Z.L., T.M. Yamamoto, A. McMellen, H. Kim, C.J. Hughes, L.J. Wheeler, M.D. Post, K. Behbakht, and B.G. Bitler, *Histone methyltransferases EHMT1 and EHMT2 (GLP/G9A) maintain PARP inhibitor resistance in high-grade serous ovarian carcinoma.* Clin Epigenetics, 2019. **11**(1): p. 165. PMID: 31775874
16. Bitler, B.G., K.M. Aird, A. Garipov, H. Li, M. Amatangelo, A.V. Kossenkov, D.C. Schultz, Q. Liu, M. Shih Ie, J.R. Conejo-Garcia, D.W. Speicher, and R. Zhang, *Synthetic lethality by targeting EZH2 methyltransferase activity in ARID1A-mutated cancers.* Nat Med, 2015. **21**(3): p. 231-8. PMID: 25686104
17. Qian, J., S. Olbrecht, B. Boeckx, H. Vos, D. Laoui, E. Etlioglu, E. Wauters, V. Pomella, S. Verbandt, P. Busschaert, A. Bassez, A. Franken, M.V. Bempt, J. Xiong, B. Weynand, Y. van Herck, A. Antoranz, F.M. Bosisio, B. Thienpont, G. Floris, I. Vergote, A. Smeets, S. Tejpar, and D. Lambrechts, *A pan-cancer blueprint of the heterogeneous tumor microenvironment revealed by single-cell profiling.* Cell Res, 2020. **30**(9): p. 745-762. PMID: 32561858
18. Tsherniak, A., F. Vazquez, P.G. Montgomery, B.A. Weir, G. Kryukov, G.S. Cowley, S. Gill, W.F. Harrington, S. Pantel, J.M. Krill-Burger, R.M. Meyers, L. Ali, A. Goodale, Y. Lee, G. Jiang, J. Hsiao, W.F.J. Gerath, S. Howell, E. Merkel, M. Ghandi, L.A. Garraway, D.E. Root, T.R. Golub, J.S. Boehm, and W.C. Hahn, *Defining a Cancer Dependency Map.* Cell, 2017. **170**(3): p. 564-576 e16. PMID: 28753430
19. Cerami, E., J. Gao, U. Dogrusoz, B.E. Gross, S.O. Sumer, B.A. Aksoy, A. Jacobsen, C.J. Byrne, M.L. Heuer, E. Larsson, Y. Antipin, B. Reva, A.P. Goldberg, C. Sander, and N. Schultz, *The cBio cancer genomics portal: an open platform for exploring multidimensional cancer genomics data.* Cancer Discov, 2012. **2**(5): p. 401-4. PMID: 22588877
20. Gao, J., B.A. Aksoy, U. Dogrusoz, G. Dresdner, B. Gross, S.O. Sumer, Y. Sun, A. Jacobsen, R. Sinha, E. Larsson, E. Cerami, C. Sander, and N. Schultz, *Integrative analysis of complex cancer genomics and clinical profiles using the cBioPortal.* Sci Signal, 2013. **6**(269): p. pl1. PMID: 23550210
21. Gunn, A. and J.M. Stark, *I-SceI-based assays to examine distinct repair outcomes of mammalian chromosomal double strand breaks.* Methods Mol Biol, 2012. **920**: p. 379-91. PMID: 22941618
22. Yamamoto, T.M., A. McMellen, Z.L. Watson, J. Aguilera, R. Ferguson, E. Nurmemmedov, T. Thakar, G.L. Moldovan, H. Kim, D.M. Cittelly, A.M. Joglar, E.P. Brennecke, H. Wilson, K. Behbakht, M.J. Sikora, and B.G. Bitler, *Activation of Wnt signaling promotes olaparib resistant ovarian cancer.* Mol Carcinog, 2019. PMID: 31219654
23. Bitler, B.G., J.P. Nicodemus, H. Li, Q. Cai, H. Wu, X. Hua, T. Li, M.J. Birrer, A.K. Godwin, P. Cairns, and R. Zhang, *Wnt5a Suppresses Epithelial Ovarian Cancer by Promoting Cellular Senescence.* Cancer Res, 2011. PMID: 21816908
24. Jassal, B., L. Matthews, G. Viteri, C. Gong, P. Lorente, A. Fabregat, K. Sidiropoulos, J. Cook, M. Gillespie, R. Haw, F. Loney, B. May, M. Milacic, K. Rothfels, C. Sevilla, V. Shamovsky, S. Shorser, T. Varusai, J. Weiser, G. Wu, L. Stein, H. Hermjakob, and P.

D'Eustachio, *The reactome pathway knowledgebase.* Nucleic Acids Res, 2020. **48**(D1): p. D498-D503. PMID: 31691815
25. Lord, C.J., S. McDonald, S. Swift, N.C. Turner, and A. Ashworth, *A high-throughput RNA interference screen for DNA repair determinants of PARP inhibitor sensitivity.* DNA Repair (Amst), 2008. **7**(12): p. 2010-9. PMID: 18832051
26. Coscia, F., K.M. Watters, M. Curtis, M.A. Eckert, C.Y. Chiang, S. Tyanova, A. Montag, R.R. Lastra, E. Lengyel, and M. Mann, *Integrative proteomic profiling of ovarian cancer cell lines reveals precursor cell associated proteins and functional status.* Nat Commun, 2016. **7**: p. 12645. PMID: 27561551
27. Chan, C.Y., K.V. Tan, and B. Cornelissen, *PARP Inhibitors in Cancer Diagnosis and Therapy.* Clin Cancer Res, 2021. **27**(6): p. 1585-1594. PMID: 33082213
28. Hurley, R.M., A.E. Wahner Hendrickson, D.W. Visscher, P. Ansell, M.I. Harrell, J.M. Wagner, V. Negron, K.M. Goergen, M.J. Maurer, A.L. Oberg, X.W. Meng, K.S. Flatten, M.J.A. De Jonge, C.D. Van Herpen, J.A. Gietema, R.H.T. Koornstra, A. Jager, M.W. den Hollander, M. Dudley, S.P. Shepherd, E.M. Swisher, and S.H. Kaufmann, *53BP1 as a potential predictor of response in PARP inhibitor-treated homologous recombination-deficient ovarian cancer.* Gynecol Oncol, 2019. **153**(1): p. 127-134. PMID: 30686551
29. Jaspers, J.E., A. Kersbergen, U. Boon, W. Sol, L. van Deemter, S.A. Zander, R. Drost, E. Wientjens, J. Ji, A. Aly, J.H. Doroshow, A. Cranston, N.M. Martin, A. Lau, M.J. O'Connor, S. Ganesan, P. Borst, J. Jonkers, and S. Rottenberg, *Loss of 53BP1 causes PARP inhibitor resistance in Brca1-mutated mouse mammary tumors.* Cancer Discov, 2013. **3**(1): p. 68-81. PMID: 23103855
30. Ali, R., M. Alabdullah, A. Alblihy, I. Miligy, K.A. Mesquita, S.Y. Chan, P. Moseley, E.A. Rakha, and S. Madhusudan, *PARP1 blockade is synthetically lethal in XRCC1 deficient sporadic epithelial ovarian cancers.* Cancer Lett, 2020. **469**: p. 124-133. PMID: 31669203
31. Litkouhi, B., J. Kwong, C.M. Lo, J.G. Smedley, 3rd, B.A. McClane, M. Aponte, Z. Gao, J.L. Sarno, J. Hinners, W.R. Welch, R.S. Berkowitz, S.C. Mok, and E.I. Garner, *Claudin-4 overexpression in epithelial ovarian cancer is associated with hypomethylation and is a potential target for modulation of tight junction barrier function using a C-terminal fragment of Clostridium perfringens enterotoxin.* Neoplasia, 2007. **9**(4): p. 304-14. PMID: 17460774
32. Coker, E.A., C. Mitsopoulos, J.E. Tym, A. Komianou, C. Kannas, P. Di Micco, E. Villasclaras Fernandez, B. Ozer, A.A. Antolin, P. Workman, and B. Al-Lazikani, *canSAR: update to the cancer translational research and drug discovery knowledgebase.* Nucleic Acids Res, 2019. **47**(D1): p. D917-D922. PMID: 30496479
33. Mizuno, H., K. Kitada, K. Nakai, and A. Sarai, *PrognoScan: a new database for meta-analysis of the prognostic value of genes.* BMC Med Genomics, 2009. **2**: p. 18. PMID: 19393097

FIGURE LEGENDS

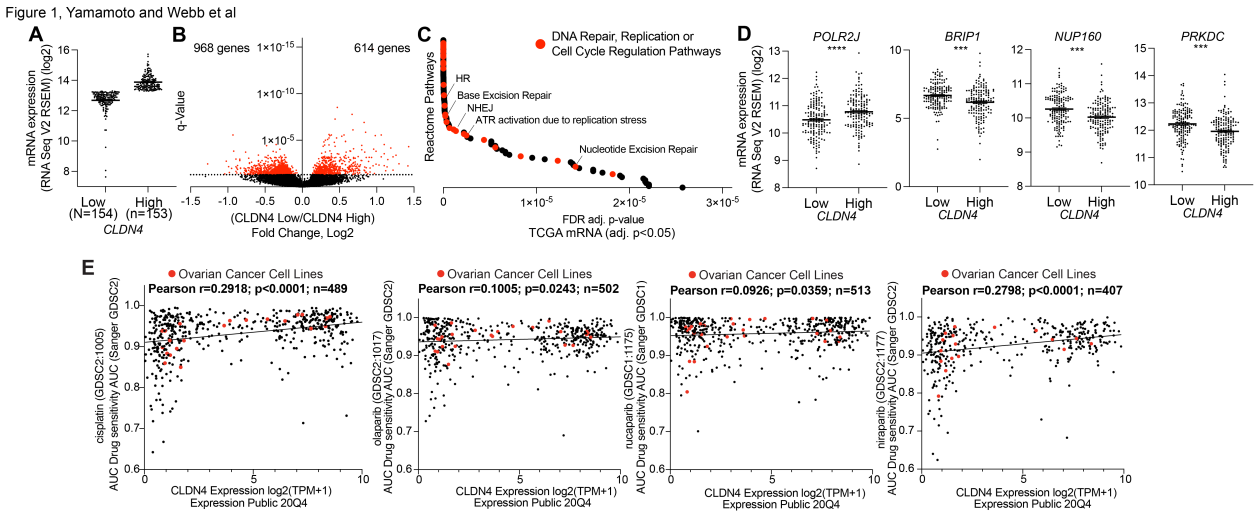

<u>Figure 1</u>: Elevated claudin-4 expression correlates to DNA repair and response to DNA damaging agents. A) Patient tumors within the TCGA (Firehose Legacy) were stratified based on the median expression of *CLDN4* expression (Low, N=154 and High, N=153). **B)** Volcano plot of 1582 differentially regulated genes between low CLDN4 expressing tumors and high CLDN4 expressing tumor. **C)** Reactome pathway analysis of 1582 genes. **D)** Representative genes from Reactome DNA repair, replication and cycle pathways. **E)** Drug sensitivity of DNA damaging agents based on *CLDN4* expression. Error bars, SEM. Statistical test, unpaired t-test with Benjamini-Hochberg multicomparison correction, ***p<0.001, ****p<0.0001.

Figure 2, Yamamoto and Webb et al 2021

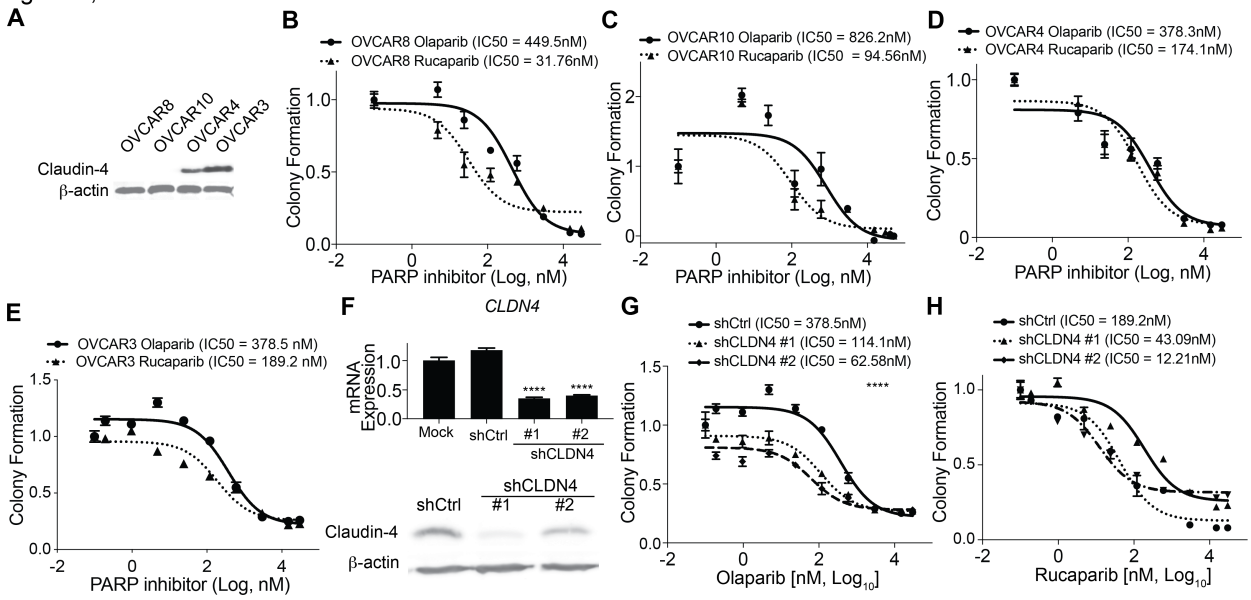

<u>Figure 2</u>: PARP inhibitor response in HGSOC cell lines with varying Claudin-4 expression. A) Claudin-4 protein expression was measured via immunoblot in a panel of HGSOC cell lines. Loading control, β-actin. Olaparib and rucaparib dose response measured via colony formation in OVCAR8 **(B)**, OVCAR10 **(C)**, OVCAR4 **(D)**, and OVCAR3 **(E)**. **F)** OVCAR3 cells transduced with shControl (shCtrl) or shCLDN4 (#1 and #2). Claudin-4 mRNA and protein levels were measured via qRT-PCR (Internal control, *B2M*) and immunoblot (Loading control, β-actin). **G)** Olaparib dose response in shCtrl and shCLDN4 cells. **H)** Rucaparib dose response in shCtrl and shCLDN4 cells. Experiments performed at least in triplicate. Error bars, SEM. Statistical test, one-way ANOVA with multicomparison correction, ***p<0.001, ****p<0.0001.

Figure 3; Yamamoto and Webb, et al.

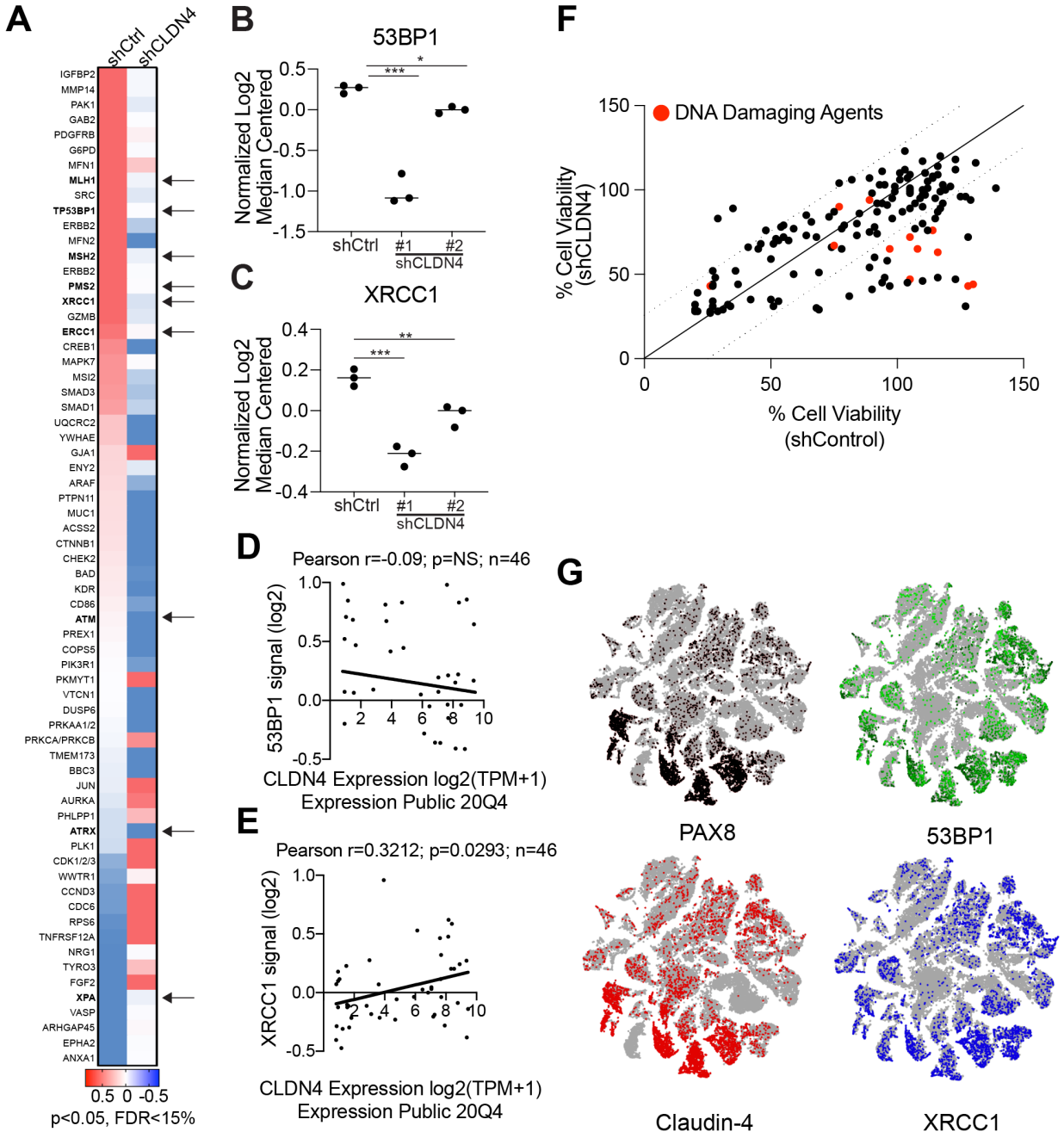

606

607 **<u>Figure 3</u>: Loss of claudin-4 downregulate DNA repair response effectors. A)** Protein

608 isolated from OVCAR3 shCtrl (n=3) and shCLDN4#1 (n=3) cells and used for Reverse Phase

609 Protein Array. Heatmap of the protein differentially regulated (p<0.05, FDR<15%). Arrows –

610 DNA repair effectors. **B)** Protein expression of 53BP1 in OVCAR3 shCtrl, shCLDN4#1, and

611 shCLDN4#2 cells. **C)** Protein expression of XRCC1 in OVCAR3 shCtrl, shCLDN4#1, and

shCLDN4#2 cells. **D)** Claudin-4 mRNA expression (x-axis) and 53BP1 protein expression (y-axis) of 46 ovarian cancer cell lines. **E)** Claudin-4 mRNA expression (x-axis) and XRCC1 protein expression (y-axis) of 46 ovarian cancer cell lines. **F)** Cell viability screen of FDA-approved oncology drugs comparing OVCAR3 shCtrl (x-axis) and shCLDN4 (y-axis). Dotted lines represent – 2 standard deviations. Red- therapies known to induce DNA damage. **G)** Single cell sequencing from 5 HGSOC tumors, *PAX8* (black, tumor cells), claudin-4 (red), *53BP1* (green), and *XRCC1* (blue). Statistical test, one way ANOVA with multicomparison correction. *$p<0.05$, **$p<0.01$, ***$p<0.001$.

Figure 4; Yamamoto and Webb, et al.

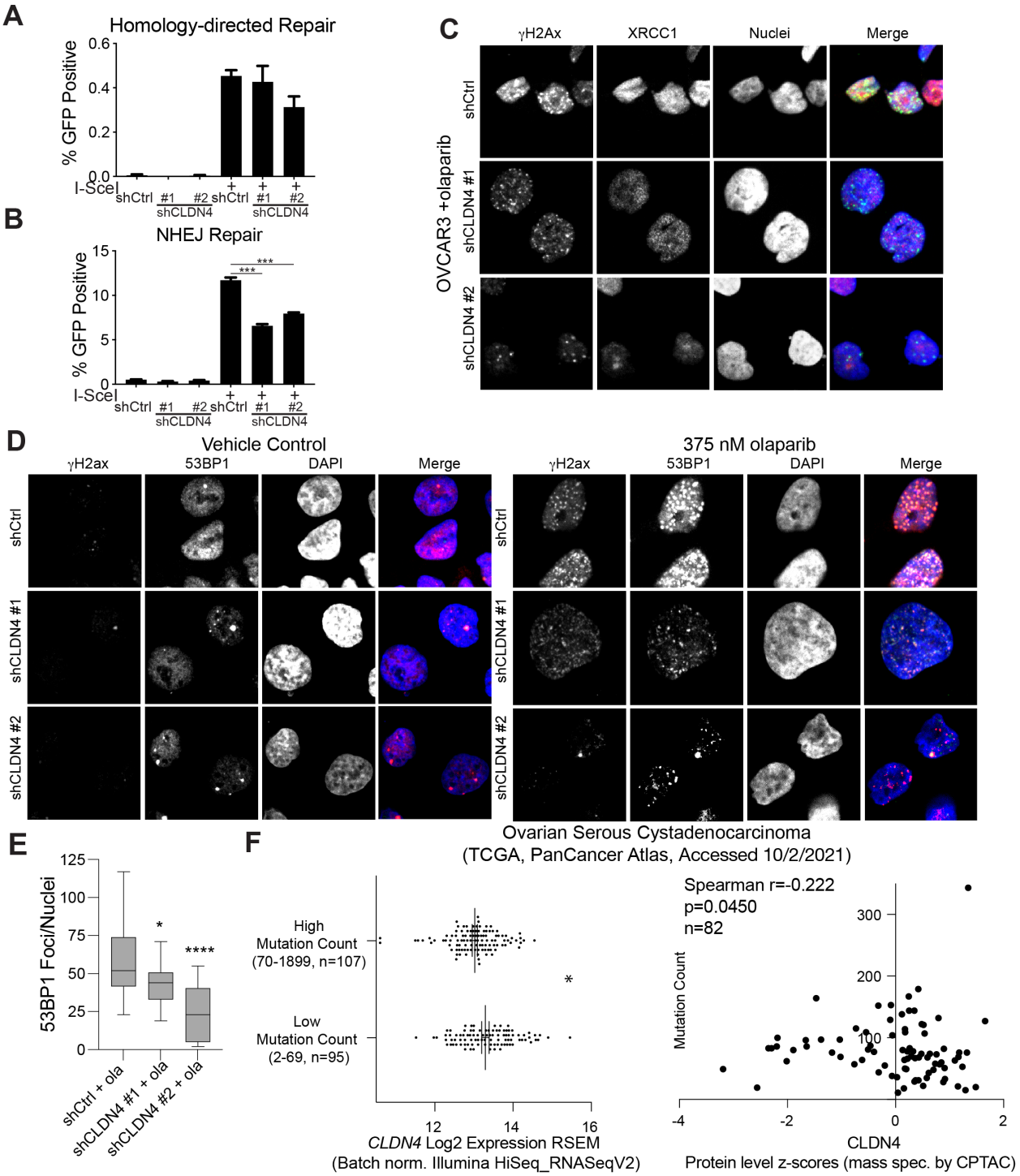

Figure 4. Claudin-4 knockdown inhibits non-homologous end joining and reduces 53BP1 foci formation. A) Homology-directed DNA repair activity measured in OVCAR3 shCtrl and shCLDN4 (#1 and #2) cells transfected without I-SceI and with I-SceI. **B)** Non-homologous end-

joining DNA repair activity measured in OVCAR3 shCtrl and shCLDN4 (#1 and #2) cells transfected without I-SceI and with I-SceI. **C)** OVCAR3 shCtrl and shCLDN4 (#1 and #2) cells treated with control [not shown] or 375 nM olaparib used for immunofluorescence against γH2ax (green) and XRCC1 (red). Nuclei stained using DAPI (blue). **D)** OVCAR3 shCtrl and shCLDN4 (#1 and #2) cells treated with vehicle control or 375 nM olaparib used for immunofluorescence against γH2ax (green) and 53BP1 (red). Nuclei stained using DAPI (blue). **E)** Same as E, quantification of 53BP1 foci per nuclei from five field of views. **F)** Low (2-69, n=95) and high (70-1899, n=107) mutation count from TCGA ovarian cancer tumors (x-axis) compared to claudin-4 mRNA expression (y-axis). Claudin-4 protein expression (CPTAC) versus Mutation count (y-axis) from 82 HGSOC TCGA tumors. Experimental performed at minimum in triplicate. Error bars, SEM. Statistical Test, one way ANOVA with multicomparison correction (A, B, E, F) or unpaired t-test (F) or Spearman Correlation (F). *p<0.05, **p<0.01, ***p<0.001, ****p<0.0001.

Figure 5; Yamamoto and Webb, et al.

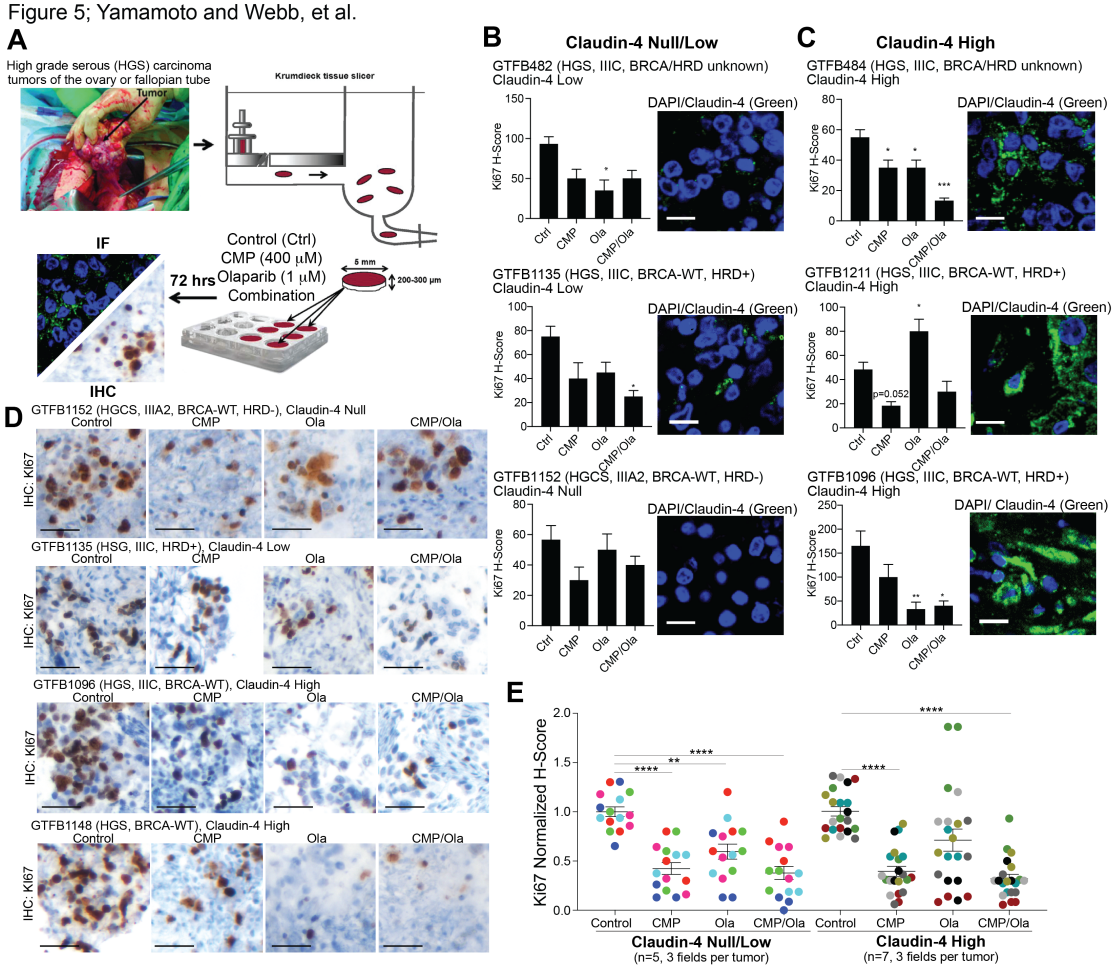

<u>Figure 5</u>: Olaparib and inhibition of claudin-4 inhibit proliferation of primary ovarian cancer tumors. A) Workflow of the ex vivo experiments using primary tumor tissue. Primary tumors were classified as claudin-4 null/low or claudin-4 high based on immunofluorescence (IF, claudin-4, green and nuclei, DAPI). IHC against Ki67 was completed in all the tumors, tumors were de-identified, and a histology score (H-score) was calculated based on intensity of Ki67 signal and percentage of tumor cells from at least three fields of view. **B)** Representative H-score and claudin-4 IF for claudin-4 null/low expressing ovarian cancer tumors. **C)** Representative H-score and claudin-4 IF for claudin-4 high expressing ovarian cancer tumors. **D)** Representative Ki67 images of claudin-4 null/low and high expressing ovarian cancer tumors (Scale bar, 50 microns). **E)** Normalized Ki67 H-score based control (Ctrl) treated tumors for all the claudin-4 null/low (N=5) and high (N=7) expressing serous ovarian tumors. Three fields from

650 each tumor were analyzed and each tumor is represented by three matched colored spots.
651 Error bars, SEM. Statistical test, one way ANOVA with multicomparison correction. *p<0.05,
652 **p<0.01, ***p<0.001, ****p<0.0001.